Eur. Phys. J. C 32, 507–528 (2004)
Digital Object Identifier (DOI) 10.1140/epjc/s2003-01463-2

THE EUROPEAN PHYSICAL JOURNAL C

Power corrections to the space-like transition form factor $F_{\eta' g^* g^*}(Q^2, \omega)$

S.S. Agaev[1,a], N.G. Stefanis[2,b]

[1] The Abdus Salam International Centre for Theoretical Physics, 34014 Trieste, Italy
[2] Institut für Theoretische Physik II, Ruhr-Universität Bochum, 44780 Bochum, Germany

Received: 19 May 2003 / Revised version: 24 October 2003 /
Published online: 8 December 2003 – © Springer-Verlag / Società Italiana di Fisica 2003

Abstract. Employing the standard hard-scattering approach (HSA) in conjunction with the running coupling (RC) method, the latter joined with the infrared renormalon calculus, we compute power-suppressed corrections $\sim 1/Q^{2n},\ n = 1, 2, \ldots$ to the massless η'-meson–virtual-gluon transition form factor (FF) $Q^2 F_{\eta' g^* g^*}(Q^2, \omega)$. Contributions to the form factor from the quark and gluon components of the η' meson are taken into account. Analytic expressions for the FFs $F_{\eta' g g^*}(Q^2, \omega = \pm 1)$ and $F_{\eta' g^* g^*}(Q^2, \omega = 0)$ are also presented, as well as Borel transforms $B[Q^2 F_{\eta' g^* g^*}](u)$ and resummed expressions. It is shown that except for $\omega = \pm 1$, 0, the Borel transform contains an infinite number of infrared renormalon poles. It is demonstrated that in the explored range of the total gluon virtuality $1\,\mathrm{GeV}^2 \leq Q^2 \leq 25\,\mathrm{GeV}^2$, power corrections found with the RC method considerably enhance the FF $F_{\eta' g^* g^*}(Q^2, \omega)$ relative to results obtained only in the context of the standard HSA with a "frozen" coupling.

1 Introduction

During the last few years the interest in theoretical investigations of the quark-gluon structure of light mesons, especially the pion, η and η' mesons, has risen due to the high-precision CLEO results on the electromagnetic $M\gamma$ transition form factors (FFs) $F_{M\gamma}(Q^2)$ [1] (with M denoting one of these mesons), as well as because of the observed very large branching ratios for the exclusive $B \to K\eta'$ and semi-inclusive $B \to \eta' X_s$ decays [2].

The data on the $\eta'\gamma$ transition FF were mainly used for extracting information concerning the η' quark component of the meson distribution amplitude (DA). Schemes and methods applied to this purpose range from light-cone perturbation-theory calculations – with the quark transverse-momentum $k_\perp$ dependence kept in the hard-scattering amplitude $T_{\mathrm{H}}(x, k_\perp, Q^2)$ of the underlying hard subprocess [3] – to the modified hard-scattering approach (mHSA) with resummed transverse-momentum effects (giving rise to Sudakov suppression factors) and such due to the intrinsic transverse momentum of the meson wave functions [4, 5], to the running coupling (RC) method, employed for the estimation of power-suppressed corrections to the $\eta'\gamma$ transition FF [6]. In these investigations, two different parameterizations were used, one employing the conventional η–η' mixing scheme with one mixing angle θ_p [3, 4, 6] for both physical states and decay constants and a second one, which considers two mixing angles θ_1 and θ_8 to parameterize the weak decay constants f_P^i ($P = \eta, \eta'$; $i = 1, 8$) of the η and η' mesons [5]. An important conclusion drawn from these investigations, irrespective of the underlying method, is that the η'-meson DA must be close to its asymptotic form and that the admixture of the first non-asymptotic term should be within the range $b_2(\mu_0^2) \simeq 0.05 \div 0.15$, b_2 being the first Gegenbauer coefficient. The CLEO data on the $\eta'\gamma$ transition and the two-angles mixing scheme were also used to estimate the allowed range of the intrinsic charm content of the η'-meson decay constant $f_{\eta'}^c$ [5]. It turned out that the value $-65\,\mathrm{MeV} \leq f_{\eta'}^c \leq 15\,\mathrm{MeV}$ does not contradict the CLEO data.

But apart from the ordinary light-quark and charm $|\eta_c'\rangle$ components, the η' meson may also contain a two-gluon valence Fock state $|gg\rangle$. Moreover, absent at the normalization point μ_0, a gluon component of the η' meson will appear in the region $Q^2 > \mu_0^2$ owing to quark–gluon mixing and renormalization-group evolution of the η'-meson DA [7–11]. This can directly contribute to the $\eta'\gamma$ transition at the next-to-leading order due to quark box diagrams and also affect the leading-order result through evolution of the quark component of the η'-meson DA. Hence, an effect of the η'-meson gluon component on the $\eta'\gamma$ transition is only mild and was therefore neglected in most theoretical investigations [3–6].

But the contribution of the gluon content of the η' meson to the two-body non-leptonic exclusive and semi-

[a] e-mail: agaev_shahin@yahoo.com
Permanent address: High Energy Physics Lab., Baku State University, Z. Khalilov St. 23, 370148 Baku, Azerbaijan
[b] e-mail: stefanis@tp2.ruhr-uni-bochum.de

inclusive decay ratios of the B meson may be sizeable. Indeed, such a mechanism to account for the observed large branching ratio [2]

$$\mathrm{Br}(B\to\eta'+X_s)=(6.2\pm1.6\pm1.3)\times10^{-4}, \qquad (1.1)$$

was proposed in [12]. In this work it was suggested that the dominant fraction of the $B\to\eta'+X_s$ decay rate appears as the result of the transition $g^*\to g\eta$ of a virtual gluon g^* from the standard model penguin diagram $b\to sg^*$. For the computation of the contribution of this mechanism to the $\mathrm{Br}(B\to\eta'+X_s)$ in [12], the $g^*g\eta'$ vertex function was approximated by the constant $H(q^2,0,m^2_{\eta'})\simeq H(0,0,m^2_{\eta'})\simeq 1.8\,\mathrm{GeV}^{-1}$, the latter being extracted from the analysis of the $J/\psi\to\eta'\gamma$ decay. Further investigations, however, demonstrated that effects of the QCD running coupling $\alpha_s(q^2)$ [13], as well as a momentum dependence of the form factor $H(q^2,0,m^2_{\eta'})$, properly taken into account, considerably reduce the contribution to (1.1) of the mechanism under consideration [14]. In order to cover the gap between theoretical predictions and experimental data in [15], a gluon fusion (spectator) mechanism was proposed. In accordance with the latter, the η' meson is produced by the fusion of a gluon from the QCD penguin diagram $b\to sg^*$ with another one emitted by the light quark inside the B meson. In this mechanism, the form factor[1] $F_{\eta' g^* g^*}({q_1}^2,q_2^2,m^2_{\eta'})$ appears owing to the $g^*g^*\to\eta'$ transition.

The same ideas form the basis for the computation of the branching ratios of various two-body non-leptonic exclusive decay modes of the B meson [16]. To account for the data on the exclusive decay $B\to K\eta'$ in [17], a mechanism was proposed, based on the assumption of a strong intrinsic charm component of the η' meson. But a more detailed analysis [18] proved that the charm content of the η' is too small ($f^c_{\eta'}\simeq-2\,\mathrm{MeV}$) to explain the observed branching ratio $\mathrm{Br}(B\to K\eta')$. The CLEO data on the B-meson non-leptonic decays that stimulated interesting theoretical works [19] remain actual until today [20].

The exclusive processes $B\to K^{(*)}\eta^{(\prime)}$ were also analyzed within the QCD factorization approach [21] and various contributions to the corresponding branching ratios were estimated [22]. In accordance with [22], the spectator mechanism and the one connected to the gluon content of the η and η' mesons are not key factors in explaining the pattern of the observed experimental data. Instead, a more important role here plays the interference (constructive or destructive) of penguin amplitudes and large radiative corrections to them, which bring the predicted branching ratios into reasonable agreement with the data.

The η'-meson–virtual-(on-shell-)gluon transition form factor $F_{\eta' g^* g^*}(q_1^2,q_2^2,m^2_{\eta'})$ is the central ingredient of analyses performed within perturbative QCD (pQCD) and hence requires further thorough investigations. Such theoretical investigations are especially important in view of contradictory predictions made for this FF in the literature [23–26]. For instance, in [23] the contribution of the gluon content of the η' meson to the form factor $F_{\eta' gg^*}(q_1^2,0,m^2_{\eta'})$ was estimated and found to be too small while $F_{\eta' gg^*}(q_1^2,0,m^2_{\eta'})$ itself is close to the form

$$F_{\eta' gg^*}(q_1^2,0,m^2_{\eta'})\simeq\frac{H(0,0,m^2_{\eta'})}{q_1^2/m^2_{\eta'}-1}=\frac{1.8}{q_1^2/m^2_{\eta'}-1}\,\mathrm{GeV}^{-1}, \qquad (1.2)$$

used in some phenomenological applications [14,15]. On the other hand, in computations of the η'-meson–virtual-gluon vertex function $F_{\eta' g^* g^*}(q_1^2,q_2^2,m^2_{\eta'})$, the gluon content of the η' meson was neglected and the asymptotic form of the DA for the quark component was employed [24]. The same vertex function $F_{\eta' g^* g^*}(q_1^2,q_2^2,m^2_{\eta'})$ was considered in [25], where both the standard HSA [27] as well as the mHSA were used, and the space- and time-like vertex functions were analyzed. Some errors made in [23] in the description of the hard-scattering amplitude of the subprocess $g+g\to g^*+g^*$ and in the definition of the evolution of the η'-meson DA were corrected in [25]. Unfortunately, also this latter work contains an incorrect expression for the gluon component $F^g_{\eta' g^* g^*}(Q^2,\omega,\eta)$ of the form factor, since it is antisymmetric under the exchange of the asymmetry parameter $\omega\leftrightarrow-\omega$ in clear conflict with Bose symmetry. More recently, in [26], the space-like form factor $F_{\eta' g^* g^*}(Q^2,\omega)$ was computed within the standard HSA. The authors of this reference performed a detailed analysis of the normalization of the gluon component of both the η'-meson DA and that of the gluon projector onto a pseudoscalar meson state.

In the present work, we investigate the massless η'-meson–virtual-gluon space-like transition form factor $F_{\eta' g^* g^*}(Q^2,\omega)$ using the framework of the standard HSA [27], as well as by applying the RC method together with the infrared (IR) renormalon calculus [28]. Our results obtained within the standard HSA are in agreement with those of [26]. But our central task here is the calculation and evolution of power-suppressed corrections $\sim 1/Q^{2n}$, $n=1,2,\ldots$ to the transition FF $Q^2F_{\eta' g^* g^*}(Q^2,\omega)$. Because in the production of the η' meson from the B decay the momentum squared of the virtual gluon can vary from $1\,\mathrm{GeV}^2$ to $25\,\mathrm{GeV}^2$, the power corrections in this domain of Q^2 are expected to play an important role. Note, however, that we elaborate only in a theoretical framework to compute power corrections for the space-like transition FF. Nevertheless, our technique can be generalized to encompass the time-like transition form factor, relevant for B-meson decays, as well. Work in this direction will be reported elsewhere.

The RC method enables us to estimate power corrections coming from the end-point $x,\,y\to0,1$ regions (for definiteness we consider two mesons in an exclusive process) in the integrals determining the amplitude for an exclusive process. It is known [27] that in order to calculate the amplitude of some hadron exclusive process, one has to perform integrations over longitudinal momentum fractions x,y of the involved partons. If one chooses the renormalization scale μ_{R}^2 in the hard-scattering amplitude T_{H} of the corresponding partonic subprocess in such a way as to minimize higher-order corrections and if one allows

[1] In this work we use the notions "vertex function" and "form factor" on the same footing

the QCD coupling constant $\alpha_{\rm s}(\mu_{\rm R}^2)$ to run, then one encounters divergences arising from the end-point $x,\ y \to 0,1$ regions. The reason is that the scale $\mu_{\rm R}^2$, as a rule, is equal to the momentum squared of the hard virtual partons, the latter carrying the strong interactions in the subprocess' Feynman diagrams [29] and, in general, depends on x and y. Within the RC method this problem is resolved by applying the IR renormalon calculus. It turns out that this treatment allows us to evaluate power-behaved corrections to the physical quantity under investigation. This method was recently used for the computation of power corrections to the electromagnetic form factors $F_{\pi,K}(Q^2)$ of the pion and the kaon [30,31] and the electromagnetic transition FFs $F_{M\gamma}(Q^2)$ [6,32] of the light pseudoscalar mesons. Power corrections to hadronic processes can also be calculated utilizing the Landau-pole free expression for the QCD coupling constant [33]. This analytic approach was used to compute in a unifying way power corrections to the electromagnetic pion form factor and to the inclusive cross section of the Drell–Yan process [34,35].

This paper is organized as follows. In Sect. 2 we briefly review η–η' mixing schemes in the flavor $SU_f(3)$ octet–singlet and the quark-flavor bases, and discuss the evolution of the quark and gluon components of the η'-meson DA with the factorization scale. The important question of the generalization of the hard-scattering amplitudes of the $\eta' g^*$ transition to the RC method case is also considered. Section 3 is devoted to a rather detailed presentation of the RC method. In Sect. 4 we compute the quark and gluon components of the transition FF $F_{\eta' g^* g^*}(Q^2,\omega)$. Section 5 contains our numerical results. Finally, in Sect. 6 we make our concluding remarks. The appendix contains additional information on the η'-meson DA.

2 Quark and gluon contributions to the η'–g^* transition form factor

In this section we consider the quark–gluon content of the η' meson, as well as the η' DA and give some general expressions for determining the $\eta' g^*$ transition form factor within both the standard HSA and the RC method.

2.1 Structure of the η' meson

The parton Fock state decomposition of the pseudoscalar $P=\eta,\ \eta'$ mesons can be generically written in the following form:

$$|P\rangle = |P_a\rangle + |P_b\rangle + |P_c\rangle + |P_g\rangle\,, \tag{2.1}$$

where $|P_a\rangle$ and $|P_b\rangle$ denote the P-meson light quarks u, d, s and $|P_c\rangle$, $|P_g\rangle$ its charm and gluon components, respectively. Fock states with additional gluons and $q\overline{q}$ quark–antiquark pairs have been omitted for simplicity.

The P-meson light-quark content $|P_a\rangle\,,\ |P_b\rangle$ can be described either in the flavor $SU_f(3)$ octet–singlet or in the quark-flavor basis. In the first scheme, the states $|P_a\rangle\,,\ |P_b\rangle$ are expressed as superpositions of the $SU_f(3)$ singlet η_1 and octet η_8 states

$$\begin{aligned}|\eta_1\rangle &= \frac{\Psi_1}{\sqrt{3}}\left|u\overline{u}+d\overline{d}+s\overline{s}\right\rangle,\\ |\eta_8\rangle &= \frac{\Psi_8}{\sqrt{6}}\left|u\overline{u}+d\overline{d}-2s\overline{s}\right\rangle,\end{aligned} \tag{2.2}$$

whereas in the quark-flavor basis, the $SU_f(3)$ strange η_s and non-strange η_q states are used, i.e.,

$$|\eta_q\rangle = \frac{\Psi_q}{\sqrt{2}}\left|u\overline{u}+d\overline{d}\right\rangle, \qquad |\eta_s\rangle = \Psi_s\left|\overline{s}\right\rangle. \tag{2.3}$$

In (2.2) and (2.3) Ψ_i denote wave functions of the corresponding parton states.

As mentioned above, the charm component of the η' meson was estimated [18,36] to be too small to considerably affect the B-meson exclusive decays. Therefore, in the present investigation we neglect the charm content of the η' meson. The maximal admixture of the two-gluon state in the η' meson was estimated to be around 26% of its content [37]. New results from the KLOE Collaboration [38] are compatible with the two-gluon contribution in the η' meson being below the level of 15%.

The pure light-quark sector of the η–η' system without charm and gluon admixtures can be treated by means of the basic states (2.2) or (2.3). In the $SU_f(3)$ octet–singlet basis, the η and η' mesons are expressed as superpositions of the η_8, η_1 states,

$$\begin{aligned}|\eta\rangle &= \cos\theta_p\,|\eta_8\rangle - \sin\theta_p\,|\eta_1\rangle\,,\\ |\eta'\rangle &= \sin\theta_p\,|\eta_8\rangle + \cos\theta_p\,|\eta_1\rangle\,.\end{aligned} \tag{2.4}$$

Here, θ_p is the mixing angle of physical states in the octet–singlet scheme. In the quark-flavor basis we get the same expressions but with θ_p replaced by the mixing angle ϕ_p of the physical states in the new basis η_q, η_s, viz.,

$$\begin{aligned}|\eta\rangle &= \cos\phi_p\,|\eta_q\rangle - \sin\phi_p\,|\eta_s\rangle\,,\\ |\eta'\rangle &= \sin\phi_p\,|\eta_q\rangle + \cos\phi_p\,|\eta_s\rangle\,.\end{aligned} \tag{2.5}$$

The η_1 and η_8 states and the mixing angle θ_p in the octet–singlet scheme can be expressed in terms of the η_q,η_s states and the mixing angle ϕ_p in the quark-flavor basis and vice versa. At the level of physical-state mixing there is no difference between the two bases (2.2) and (2.3). This only appears when one parameterizes the decay constants f_P^i of the $P=\eta$ and η' mesons in terms of

$$\left\langle 0|J^i_{\mu 5}|P\right\rangle = {\rm i} f_P^i p_\mu,$$

where $J^i_{\mu 5}$ is the axial-vector current with $i=q,\,s$ or $i=1,\,8$. In the quark-flavor basis the decay constants $f_P^{q(s)}$ follow with great accuracy the pattern of the state mixing [39,40]

$$\begin{aligned}f_\eta^q &= f_q\cos\phi_p, \quad f_\eta^s = -f_s\sin\phi_p,\\ f_{\eta'}^q &= f_q\sin\phi_p, \quad f_{\eta'}^s = f_s\cos\phi_p.\end{aligned} \tag{2.6}$$

The situation with the parameterization of the decay constants in the octet–singlet basis is different. In this case, in order to take into account the flavor $SU_f(3)$ symmetry breaking effects, a two mixing-angles scheme for the decay constants $f_P^{1(8)}$ was introduced [41]:

$$f_\eta^8 = f_8\cos\theta_8, \quad f_\eta^1 = -f_1\sin\theta_1,$$
$$f_{\eta'}^8 = f_8\sin\theta_8, \quad f_{\eta'}^1 = f_1\cos\theta_1. \tag{2.7}$$

The mixing angles θ_1 and θ_8 differ from each other and also from the state mixing angle θ_p. Nevertheless, in some phenomenological applications the conventional octet–singlet mixing scheme, that is the scheme with one mixing angle and with the assumption of the equality $\theta_1 = \theta_8 = \theta_p$ is used. In the investigation of physical processes both the octet–singlet and the quark-flavor bases may be used. A detailed analysis of the η–η' mixing problems and further references can be found in [42].

In our present work we choose the quark-flavor basis (2.3) and the mixing scheme (2.5). In this scheme, the decay constants f_q and f_s and the mixing angle ϕ_p have the following values [40, 42]:

$$f_q = (1.07\pm 0.02)f_\pi, \quad f_s = (1.34\pm 0.06)f_\pi,$$
$$\phi_p = 39.3^\circ \pm 1.0^\circ$$

with $f_\pi = 0.131\,\mathrm{GeV}$ being the pion weak decay constant. The KLOE result for $\phi_p = (41.8^{\circ+1.9^\circ}_{-1.6^\circ})$ [38] is slightly shifted towards larger values, but it still does not contradict the average value $\phi_p = 39.3^\circ \pm 1.0^\circ$. In our numerical computations we shall use the central values of the constants shown above.

The singlet part of the η'-meson DA[2] $\phi(x,\mu^2)$ was obtained in [9–11] by solving the evolution equation and was found to depend on both functions $\phi^q(x,\mu^2)$ and $\phi^g(x,\mu^2)$. These functions denote the quark and gluon components of the η'-meson DA, respectively, and satisfy the symmetry and antisymmetry conditions,

$$\phi^q(x,\mu^2) = \phi^q(1-x,\mu^2), \quad \phi^g(x,\mu^2) = -\phi^g(1-x,\mu^2). \tag{2.8}$$

This follows from the symmetry properties of the DA of the two-particle bound state of a neutral pseudoscalar meson and is in fact enough to obtain general expressions for the η'-meson–virtual-gluon transition form factor. The evolution of the functions $\phi^q(x,\mu^2)$ and $\phi^g(x,\mu^2)$ with the scale μ^2, as well as their dependence on the constants f_q, f_s and ϕ_p will be considered in Sect. 2.3.

2.2 The η'–g^* transition form factor $F_{\eta' g^* g^*}(Q^2,\omega)$

The massless η'-meson–virtual-gluon transition form factor,

$$F_{\eta' g^* g^*}(Q^2,\omega) = F^q_{\eta' g^* g^*}(Q^2,\omega) + F^g_{\eta' g^* g^*}(Q^2,\omega), \tag{2.9}$$

can be defined in terms of the invariant amplitude

$$M = M^q + M^g, \tag{2.10}$$

for the process

$$\eta'(P) \to g^*(q_1) + g^*(q_2), \tag{2.11}$$

in the following way:

$$M^{q(g)} = -\mathrm{i}F^{q(g)}_{\eta' g^* g^*}(Q^2,\omega)\delta_{ab}\epsilon^{\mu\nu\rho\sigma}\epsilon^{a*}_\mu\epsilon^{b*}_\nu q_{1\rho}q_{2\sigma}. \tag{2.12}$$

In (2.12) ϵ^a_μ, ϵ^b_ν and q_1, q_2 are, respectively, the polarization vectors and four-momenta of the two gluons. Because we study only the space-like FF, q_1^2 and q_2^2 obey the constraints $Q_1^2 = -q_1^2 \geq 0$, $Q_2^2 = -q_2^2 > 0$ and $Q_1^2 = -q_1^2 > 0$, $Q_2^2 = -q_2^2 \geq 0$. The form factor $F_{\eta' g^* g^*}(Q^2,\omega)$ depends on the total gluon virtuality Q^2 and the asymmetry parameter ω, defined by

$$Q^2 = Q_1^2 + Q_2^2, \quad \omega = \frac{Q_1^2 - Q_2^2}{Q^2}. \tag{2.13}$$

The asymmetry parameter ω varies in the region $-1 \leq \omega \leq 1$. The value $\omega = \pm 1$ corresponds to the η'-meson–on-shell-gluon transition and the value $\omega = 0$ to the situation when the gluons have equal virtualities $Q_1^2 = Q_2^2$.

In accordance with the factorization theorems of pQCD at high momentum transfer, the FFs $F^{q(g)}_{\eta' g^* g^*}(Q^2,\omega)$ are given by the expressions

$$F^q_{\eta' g^* g^*}(Q^2,\omega) \tag{2.14}$$
$$= \left[T^q_{\mathrm{H}}(x,Q^2,\omega,\mu_{\mathrm{F}}^2) + T^q_{\mathrm{H}}(\overline{x},Q^2,\omega,\mu_{\mathrm{F}}^2)\right] \otimes \phi^q(x,\mu_{\mathrm{F}}^2)$$

and

$$F^g_{\eta' g^* g^*}(Q^2,\omega) \tag{2.15}$$
$$= \left[T^g_{\mathrm{H}}(x,Q^2,\omega,\mu_{\mathrm{F}}^2) - T^g_{\mathrm{H}}(\overline{x},Q^2,\omega,\mu_{\mathrm{F}}^2)\right] \otimes \phi^g(x,\mu_{\mathrm{F}}^2).$$

Here, $\overline{x} \equiv 1-x$ and μ_{F}^2 represents the factorization scale. In (2.14) and (2.15) we have used the notation

$$T_{\mathrm{H}}(x,Q^2,\omega,\mu_{\mathrm{F}}^2) \otimes \phi(x,\mu_{\mathrm{F}}^2)$$
$$= \int_0^1 T_{\mathrm{H}}(x,Q^2,\omega,\mu_{\mathrm{F}}^2)\phi(x,\mu_{\mathrm{F}}^2)\mathrm{d}x. \tag{2.16}$$

The sum

$$T^q_{\mathrm{H}}(x,Q^2,\omega,\mu_{\mathrm{F}}^2) + T^q_{\mathrm{H}}(\overline{x},Q^2,\omega,\mu_{\mathrm{F}}^2) \tag{2.17}$$

and the difference

$$T^g_{\mathrm{H}}(x,Q^2,\omega,\mu_{\mathrm{F}}^2) - T^g_{\mathrm{H}}(\overline{x},Q^2,\omega,\mu_{\mathrm{F}}^2) \tag{2.18}$$

represent the hard-scattering amplitudes for the subprocesses $q+\overline{q} \to g^* + g^*$ and $g+g \to g^* + g^*$, respectively. The Feynman diagrams contributing at the leading order to these subprocesses' amplitudes are depicted in Figs. 1 and 2.

[2] The octet component of the η'-meson DA is irrelevant for our present investigation and will not be considered here. In what follows we refer to the singlet part of the η'-meson DA as being the η'-meson DA.

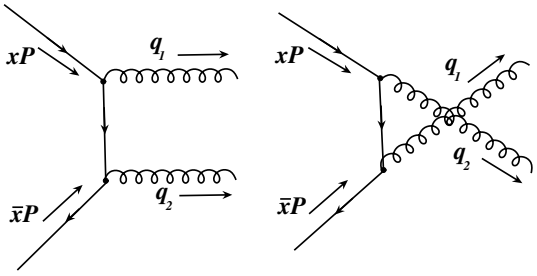

Fig. 1. Leading-order Feynman diagrams contributing to the hard-scattering subprocess $q+\overline{q}\to g^*+g^*$

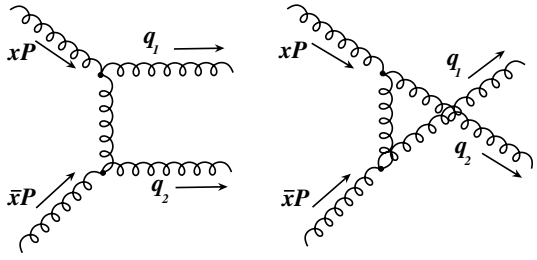

Fig. 2. Feynman diagrams contributing at leading order to the subprocess $g+g\to g^*+g^*$

In what follows, we omit the subscript H in (2.17) and (2.18) and introduce instead the notation

$$T_1^{q(g)}(x,Q^2,\omega,\mu_{\rm F}^2)=T_{\rm H}^{q(g)}(x,Q^2,\omega,\mu_{\rm F}^2),$$
$$T_2^{q(g)}(x,Q^2,\omega,\mu_{\rm F}^2)=T_{\rm H}^{q(g)}(\overline{x},Q^2,\omega,\mu_{\rm F}^2).$$

In leading order of pQCD, we get for the hard-scattering amplitudes $T_1^{q(g)}$ and $T_2^{q(g)}$ of the massless η'-meson–virtual-gluon transition FF the following expressions:

$$T_1^q(x,Q^2,\omega,\mu_{\rm R}^2)=-\frac{4\pi}{3Q^2}\frac{\alpha_{\rm s}(\mu_{\rm R}^2)}{(1+\omega)x+(1-\omega)\overline{x}},$$
$$T_2^q(x,Q^2,\omega,\overline{\mu}_{\rm R}^2)=-\frac{4\pi}{3Q^2}\frac{\alpha_{\rm s}(\overline{\mu}_{\rm R}^2)}{(1+\omega)\overline{x}+(1-\omega)x} \quad (2.19)$$

and

$$T_1^g(x,Q^2,\omega,\mu_{\rm R}^2)=\frac{\pi\alpha_{\rm s}(\mu_{\rm R}^2)}{Q^2 n_f}\frac{(1+\omega)x+(1-\omega)\overline{x}}{\omega\left[(1+\omega)\overline{x}+(1-\omega)x\right]},$$
$$T_2^g(x,Q^2,\omega,\overline{\mu}_{\rm R}^2)=\frac{\pi\alpha_{\rm s}(\overline{\mu}_{\rm R}^2)}{Q^2 n_f}\frac{(1+\omega)\overline{x}+(1-\omega)x}{\omega\left[(1+\omega)x+(1-\omega)\overline{x}\right]}. \quad (2.20)$$

In deriving the hard-scattering amplitudes $T_{1(2)}^g(x,Q^2,\omega,\mu_{\rm R}^2)$ (they are the object of contradictory conclusions in the literature [25,26]), the following projection operator of the η'-meson onto the two-gluon state has been used:

$$P_{\mu\nu,ab}=\mathrm{i}\frac{\delta_{ab}}{\sqrt{6}\sqrt{n_f}}\frac{\epsilon_{\mu\nu\gamma\delta}q_1^\gamma q_2^\delta}{\omega Q^2}.$$

Note that in the limit $\omega=0$ the difference $T_1^g-T_2^g$, being the physical hard-scattering amplitude, is singularity free (see (4.25) below). In the expressions above, $\alpha_{\rm s}(\mu^2)$ is the QCD coupling constant in the two-loop approximation defined by

$$\alpha_{\rm s}(\mu^2)=\frac{4\pi}{\beta_0\ln(\mu^2/\Lambda^2)}\left[1-\frac{2\beta_1}{\beta_0^2}\frac{\ln\ln(\mu^2/\Lambda^2)}{\ln(\mu^2/\Lambda^2)}\right], \quad (2.21)$$

with β_0 and β_1 being the one- and two-loop coefficients of the QCD beta function:

$$\beta_0=11-\frac{2}{3}n_f,\quad \beta_1=51-\frac{19}{3}n_f. \quad (2.22)$$

In (2.20), (2.21), and (2.22) $\Lambda=0.3\,\mathrm{GeV}$ is the QCD scale parameter and n_f is the number of active quark flavors.

The physical quantity $F_{\eta' g^* g^*}(Q^2,\omega)$, represented at sufficiently high Q^2 by the factorization formulas (2.14), (2.15), is independent of the renormalization scheme and the renormalization and factorization scales $\mu_{\rm R}^2$ ($\overline{\mu}_{\rm R}^2$) and $\mu_{\rm F}^2$. Truncation of the perturbation series of $F_{\eta' g^* g^*}(Q^2,\omega)$ at any finite order causes a residual dependence on the scheme as well as on these scales. At the leading order of pQCD, the hard-scattering amplitude does not depend on the factorization scale $\mu_{\rm F}^2$ but depends implicitly on the renormalization scale $\mu_{\rm R}^2$ through $\alpha_{\rm s}(\mu_{\rm R}^2)$.[3] An explicit dependence of the function $T_{\rm H}$ on $\mu_{\rm R}^2$ and $\mu_{\rm F}^2$ appears at $O(\alpha_{\rm s})$ due to QCD corrections. As the scales $\mu_{\rm R}^2$ and $\mu_{\rm F}^2$ are independent of each other and can be chosen separately, we adopt in this work the natural and widely used "default" choice for the factorization scale $\mu_{\rm F}^2=Q^2$ and omit in what follows a dependence of the hard-scattering amplitude on $\mu_{\rm F}^2$ (see (2.19) and (2.20)). For a more detailed discussion of these questions, we refer the interested reader to [43].

In the standard HSA with a "frozen" coupling constant [27] one sets the renormalization scale $\mu_{\rm R}^2=\overline{\mu}_{\rm R}^2=Q^2$, simplifying the calculation of the vertex function $F_{\eta' g^* g^*}(Q^2,\omega)$ considerably. In this approach the hard-scattering amplitudes $T_{1,2}^{q(g)}$ and hence the quark and gluon components of the vertex function $F_{\eta' g^* g^*}(Q^2,\omega)$ possess symmetry features pertaining to the RC method. Indeed, it is not difficult to see that

$$T_{1(2)}^q(\overline{x},Q^2,\omega)=T_{2(1)}^q(x,Q^2,\omega),$$
$$T_{1(2)}^q(x,Q^2,-\omega)=T_{2(1)}^q(x,Q^2,\omega) \quad (2.23)$$

and

$$T_{1(2)}^g(\overline{x},Q^2,\omega)=T_{2(1)}^g(x,Q^2,\omega),$$
$$T_{1(2)}^g(x,Q^2,-\omega)=-T_{2(1)}^g(x,Q^2,\omega). \quad (2.24)$$

Using (2.8) and (2.23), we then find

$$\begin{aligned}&F_{\eta' g^* g^*}^q(Q^2,\omega)\\&=T_1^q(x,Q^2,\omega)\otimes\phi^q(x,Q^2)+(\omega\leftrightarrow-\omega)\\&=2T_1^q(x,Q^2,\omega)\otimes\phi^q(x,Q^2).\end{aligned} \quad (2.25)$$

[3] Similar arguments hold for the scale $\overline{\mu}_{\rm R}^2$

In a similar manner, using (2.8) and (2.24), one can demonstrate that the following equalities hold:

$$\begin{aligned} &F^g_{\eta' g^* g^*}(Q^2,\omega) \\ &= T^g_1(x,Q^2,\omega)\otimes\phi^g(x,Q^2) + (\omega\leftrightarrow-\omega) \\ &= 2T^g_1(x,Q^2,\omega)\otimes\phi^g(x,Q^2). \end{aligned} \tag{2.26}$$

From (2.25) and (2.26) it follows that

$$\begin{aligned} F^q_{\eta' g^* g^*}(Q^2,\omega) &= F^q_{\eta' g^* g^*}(Q^2,-\omega), \\ F^g_{\eta' g^* g^*}(Q^2,\omega) &= F^g_{\eta' g^* g^*}(Q^2,-\omega). \end{aligned} \tag{2.27}$$

In pQCD calculations higher-order corrections to various physical processes, are, in general, large and in order to improve the convergence of the corresponding perturbative series, different methods have been proposed. In exclusive processes – considering the pion electromagnetic form factor as a prominent example – the next-to-leading order $O(\alpha_s)$ correction contains logarithmic terms $\sim \ln(Q^2\overline{x}y/\mu_R^2)$ (or $\sim \ln(Q^2xy/\mu_R^2)$) [44,45], which can be entirely or partly eliminated by a proper choice of the renormalization scale μ_R^2 ($\overline{\mu}_R^2$). This can be achieved by taking as a renormalization scale $\mu_R^2 = Q^2\overline{x}y$ [$\overline{\mu}_R^2 = Q^2xy$] or $\mu_R^2 = Q^2\overline{x}/2$ [$\overline{\mu}_R^2 = Q^2x/2$]. The renormalization scale enters into the pQCD expression not only via logarithmic terms, but also through the argument of the running coupling $\alpha_s(\mu_R^2)$. In order to calculate the amplitude of an exclusive process, an integration in corresponding integrals over the longitudinal momentum fractions of the quarks and gluons in the involved hadrons has to be carried out. Thus, in the pion electromagnetic FF calculations, the integration over the variables x and y has to be performed. Traditionally, to avoid problems associated with singularities of $\alpha_s(\mu_R^2)$, one "freezes" the running coupling by replacing x and y, e.g., by their mean values $x\to\langle x\rangle = 1/2,\ y\to\langle y\rangle = 1/2$ in the argument of $\alpha_s(\mu_R^2)$ and performs then the calculation with $\alpha_s(Q^2/4)$ [44]. Recently, the RC method for the calculation of various exclusive processes with $\alpha_s(\mu_R^2)$ was proposed. Within this framework, one expresses the running coupling $\alpha_s(Q^2x)$ in terms of $\alpha_s(Q^2)$ by employing the renormalization-group equation and performs the integration over $x(y)$ using the principal value prescription. This allows one to estimate power-suppressed corrections to the process under consideration towards the end-point region of phase space, thus improving the agreement of QCD theoretical predictions with experimental data. An alternative option to calculate power-behaved contributions with their coefficients would be to use the analytic perturbation theory [33] along the lines proposed in [34,35]. Next-to-leading order corrections are known for only a few exclusive processes [44–46]. In general, the renormalization scale μ_R^2 may be taken equal or proportional to the square of the four-momentum q^2 of the virtual parton(s) mediating the strong interaction in corresponding leading-order Feynman diagrams.

For the η'-meson–on-shell gluon transition (i.e., for $\omega = \pm1$), we adopt in this paper the choice

$$\mu_R^2 = Q^2x, \quad \overline{\mu}_R^2 = Q^2\overline{x}. \tag{2.28}$$

The renormalization scales (2.28) are equal to the momentum squared $|q^2|$ of the virtual partons (gluon or quark) in the corresponding Feynman diagrams. In the general case ($\omega \neq \pm1$), the absolute value of the square of the four-momenta q^2 of the virtual partons depends on both the total gluon virtuality Q^2 and the asymmetry parameter ω. However, for the sake of simplifying the calculations and to avoid problems related to the appearance of two parameters Q^2 and ω in the argument of α_s, we shall use a renormalization scale of the form given in (2.28). This choice is justified from the physical point of view because those parts of the scales $\sim Q^2x,\ \sim Q^2\overline{x}$ are exactly responsible for the power corrections $\sim 1/Q^{2n}$, $n = 1, 2, \ldots$ to the form factor $Q^2F_{\eta' g^* g^*}(Q^2,\omega)$ which we are going to compute.

The next problem then is how to generalize (2.19) and (2.20) in such a way that the corresponding hard-scattering amplitudes $T^{q(g)}_{1(2)}$ and the quark and gluon components of the vertex function will obey (2.23)–(2.27). For this purpose, we symmetrize the functions $T^{q(g)}_{1(2)}(x,Q^2,\omega,\mu_R^2(\overline{\mu}_R^2))$ by exchanging $\mu_R^2 \leftrightarrow \overline{\mu}_R^2$ to obtain

$$\begin{aligned} T^q_1(x,Q^2,\omega) &= \frac{1}{2}\left[T^q_1(x,Q^2,\omega,\mu_R^2) + T^q_1(x,Q^2,\omega,\overline{\mu}_R^2)\right] \\ &= -\frac{2\pi}{3Q^2}\frac{\alpha_s(Q^2x)+\alpha_s(Q^2\overline{x})}{(1+\omega)x+(1-\omega)\overline{x}}, \\ T^q_2(x,Q^2,\omega) &= \frac{1}{2}\left[T^q_2(x,Q^2,\omega,\overline{\mu}_R^2) + T^q_2(x,Q^2,\omega,\mu_R^2)\right] \\ &= -\frac{2\pi}{3Q^2}\frac{\alpha_s(Q^2x)+\alpha_s(Q^2\overline{x})}{(1+\omega)\overline{x}+(1-\omega)x} \end{aligned} \tag{2.29}$$

and

$$\begin{aligned} &T^g_1(x,Q^2,\omega) \\ &= \frac{1}{2}\left[T^g_1(x,Q^2,\omega,\mu_R^2) + T^g_1(x,Q^2,\omega,\overline{\mu}_R^2)\right] \\ &= \frac{\pi}{2Q^2n_f}\left[\alpha_s(Q^2x)+\alpha_s(Q^2\overline{x})\right] \\ &\quad\times\frac{(1+\omega)x+(1-\omega)\overline{x}}{\omega\left[(1+\omega)\overline{x}+(1-\omega)x\right]}, \\ &T^g_2(x,Q^2,\omega) \\ &= \frac{1}{2}\left[T^g_2(x,Q^2,\omega,\overline{\mu}_R^2) + T^g_2(x,Q^2,\omega,\mu_R^2)\right] \\ &= \frac{\pi}{2Q^2n_f}\left[\alpha_s(Q^2x)+\alpha_s(Q^2\overline{x})\right] \\ &\quad\times\frac{(1+\omega)\overline{x}+(1-\omega)x}{\omega\left[(1+\omega)x+(1-\omega)\overline{x}\right]}. \end{aligned} \tag{2.30}$$

In the "frozen" coupling-constant approximation Q^2x, $Q^2\overline{x}\to Q^2$, (2.29) and (2.30) coincide with expressions (2.19) and (2.20). It is also not difficult to verify that the hard-scattering amplitudes $T^{q(g)}_{1(2)}(x,Q^2,\omega)$(2.29) and (2.30) satisfy (2.23) and (2.24). As a result, (2.25)–(2.27) remain valid also within the RC method.

2.3 Quark and gluon components of the η' meson distribution amplitude

The important input information needed for the computation of the form factor $F_{\eta' g^* g^*}(Q^2,\omega)$ are the DAs of the quark and gluon components of the η' meson, namely, the functions $\phi^q(x,Q^2)$ and $\phi^g(x,Q^2)$. In general, a meson DA is a function containing all non-perturbative, long-distance effects, which cannot be calculated by employing perturbative QCD tools. Its dependence on x (or its shape) has to be deduced from experimental data or found using some non-perturbative methods, for example, QCD sum-rules (see, e.g., [47]). In contrast, the evolution of the DA with the factorization scale Q^2 is governed by pQCD.

The evolution equation for the DA of a flavor singlet pseudoscalar meson was derived and solved in [9–11]. It turned out that due to mixing of the quark–antiquark and two-gluon components of the meson DA, the evolution equation has a (2×2) matrix form. The anomalous dimensions matrix, which enters into the evolution equation at the one-loop order, has the following components [9–11] (see also [48]):

$$\gamma_{qq}^n = C_{\rm F}\left[3+\frac{2}{(n+1)(n+2)}-4\sum_{j=1}^{n+1}\frac{1}{j}\right],$$
$$\gamma_{gg}^n = N_c\left[\frac{\beta_0}{N_c}+\frac{8}{(n+1)(n+2)}-4\sum_{j=1}^{n+1}\frac{1}{j}\right], \quad (2.31)$$
$$\gamma_{qg}^n = \frac{12n_f}{(n+1)(n+2)}, \quad \gamma_{gq}^n = C_{\rm F}\frac{n(n+3)}{3(n+1)(n+2)},$$

where $N_c=3$ and $C_{\rm F}=4/3$ is the group theoretical factor for $SU_c(3)$. The anomalous dimensions matrix has the eigenvalues

$$\gamma_{\pm}^n = \frac{1}{2}\left[\gamma_{qq}^n+\gamma_{gg}^n \pm \sqrt{(\gamma_{qq}^n-\gamma_{gg}^n)^2+4\gamma_{qg}^n\gamma_{gq}^n}\right]. \quad (2.32)$$

The solutions of the evolution equation for the quark and gluon components of the DA have, in general, the form

$$\phi^q(x,Q^2) = 6Cx\overline{x} \times\left\{1+\sum_{k=2,4,\ldots}^{\infty}\left[B_n^q\left(\frac{\alpha_{\rm s}(\mu_0^2)}{\alpha_{\rm s}(Q^2)}\right)^{\frac{\gamma_+^n}{\beta_0}}+\rho_n^g B_n^g\left(\frac{\alpha_{\rm s}(\mu_0^2)}{\alpha_{\rm s}(Q^2)}\right)^{\frac{\gamma_-^n}{\beta_0}}\right]\times C_n^{3/2}(x-\overline{x})\right\} \quad (2.33)$$

and

$$\phi^g(x,Q^2) = Cx\overline{x} \times\sum_{k=2,4,\ldots}^{\infty}\left[\rho_n^q B_n^q\left(\frac{\alpha_{\rm s}(\mu_0^2)}{\alpha_{\rm s}(Q^2)}\right)^{\frac{\gamma_+^n}{\beta_0}}+B_n^g\left(\frac{\alpha_{\rm s}(\mu_0^2)}{\alpha_{\rm s}(Q^2)}\right)^{\frac{\gamma_-^n}{\beta_0}}\right]\times C_{n-1}^{5/2}(x-\overline{x}) \quad (2.34)$$

with the constant C being defined as

$$C=\sqrt{2}f_q\sin\phi_p+f_s\cos\phi_p.$$

In (2.33) and (2.34) $C_n^{3/2}(z)$ and $C_n^{5/2}(z)$ are Gegenbauer polynomials, calculable using the recurrence formula [49]

$$(n+1)C_{n+1}^{\nu}(z) = 2(n+\nu)zC_n^{\nu}(z)-(n+2\nu-1)C_{n-1}^{\nu}(z), \quad (2.35)$$
$$C_0^{\nu}(z)=1, \quad C_1^{\nu}(z)=2\nu z.$$

The parameters ρ_n^q and ρ_n^g are determined in terms of the anomalous dimensions matrix elements

$$\rho_n^q = 6\frac{\gamma_+^n-\gamma_{qq}^n}{\gamma_{gq}^n}, \quad \rho_n^g = \frac{1}{6}\frac{\gamma_{gq}^n}{\gamma_-^n-\gamma_{qq}^n}. \quad (2.36)$$

In (2.33) and (2.34) $\mu_0=1\,$GeV is the normalization point, at which the free input parameters B_n^q, B_n^g in the DAs $\phi^q(x,Q^2)$ and $\phi^g(x,Q^2)$ have to be fixed. Exactly these parameters determine the shape of the DAs.

For all $n\geq 2$, the eigenvalues $\gamma_{\pm}^n<0$ and their absolute values increase with n. Hence, in the asymptotic limit $Q^2\to\infty$, one has

$$\left(\frac{\alpha_{\rm s}(\mu_0^2)}{\alpha_{\rm s}(Q^2)}\right)^{\frac{\gamma_+^n(\gamma_-^n)}{\beta_0}} \sim \ln\left(Q^2/\Lambda^2\right)^{\frac{\gamma_+^n(\gamma_-^n)}{\beta_0}}\to 0$$

and therefore only the quark component of the η'-meson DA survives, evolving to its asymptotic form, whereas the gluon DA in this limit vanishes,

$$\phi^q(x,Q^2)\stackrel{Q^2\to\infty}{\longrightarrow} 6Cx\overline{x}, \quad \phi^g(x,Q^2)\stackrel{Q^2\to\infty}{\longrightarrow} 0. \quad (2.37)$$

In this work, we shall use the η'-meson DA that contains only the first non-asymptotic terms. In other words, we suggest that in (2.33) and (2.34) $B_2^q\neq 0$, $B_2^g\neq 0$ and $B_n^q=B_n^g=0$ for all $n\geq 4$. The numerical values of the relevant parameters for $n_f=3$ are

$$\gamma_{qq}^2=-\frac{50}{9}, \quad \gamma_{gg}^2=-11, \quad \gamma_{gq}^2=\frac{10}{27}, \quad \gamma_{qg}^2=3,$$
$$\gamma_+^2\simeq-\frac{48}{9}, \quad \gamma_-^2\simeq-\frac{101}{9}, \quad \rho_2^q\simeq\frac{16}{5}, \quad \rho_2^g\simeq-\frac{1}{90}. \quad (2.38)$$

Taking into account (2.38) and the expressions for the required Gegenbauer polynomials

$$C_2^{3/2}(x-\overline{x}) = \frac{3}{2}\left[5(x-\overline{x})^2-1\right] = 6\left(1-5x\overline{x}\right),$$
$$C_1^{5/2}(x-\overline{x}) = 5(x-\overline{x}),$$

we finally recast the η'-meson quark and gluon DAs into the more suitable (for our purposes) forms,

$$\phi^q(x,Q^2) = 6Cx\overline{x}\left[1+A(Q^2)-5A(Q^2)x\overline{x}\right],$$

$$\phi^g(x,Q^2) = Cx\overline{x}(x-\overline{x})B(Q^2). \tag{2.39}$$

In these expressions the functions $A(Q^2)$ and $B(Q^2)$ are defined by

$$A(Q^2) = 6B_2^q\left(\frac{\alpha_{\rm s}(Q^2)}{\alpha_{\rm s}(\mu_0^2)}\right)^{\frac{48}{81}} - \frac{B_2^g}{15}\left(\frac{\alpha_{\rm s}(Q^2)}{\alpha_{\rm s}(\mu_0^2)}\right)^{\frac{101}{81}},$$

$$B(Q^2) = 16B_2^q\left(\frac{\alpha_{\rm s}(Q^2)}{\alpha_{\rm s}(\mu_0^2)}\right)^{\frac{48}{81}} + 5B_2^g\left(\frac{\alpha_{\rm s}(Q^2)}{\alpha_{\rm s}(\mu_0^2)}\right)^{\frac{101}{81}}. \tag{2.40}$$

The η'-meson quark and gluon DAs for $n_f = 4$ are given in the appendix. Equations (2.39), (2.40), and (A.1) contain all necessary information about the singlet part of the η'-meson DA.

3 Running coupling method and power-suppressed corrections

To compute the η'-meson–virtual-gluon transition form factor $F_{\eta' g^* g^*}(Q^2,\omega)$, we have to perform in (2.14) and (2.15) the integration over x by inserting the explicit expressions for the hard-scattering amplitudes $T_{1,2}^{q(g)}(x,Q^2,\omega)$ and the η'-meson quark and gluon DAs, and retain the x dependence of the coupling $\alpha_{\rm s}(Q^2x)$ $[\alpha_{\rm s}(Q^2\overline{x})]$. Such calculations lead to divergent integrals because the running coupling $\alpha_{\rm s}(Q^2x)$ $[\alpha_{\rm s}(Q^2\overline{x})]$ suffers from an infrared singularity in the limit $x \to 0$ $[x \to 1]$. This means that in order to carry out computations with the running coupling, some procedure for its regularization in the end-point $x \to 0,\, 1$ regions has to be adopted.

As a first step in this direction, we express the running coupling $\alpha_{\rm s}(Q^2x)$ in terms of $\alpha_{\rm s}(Q^2)$, employing the renormalization-group equation

$$\frac{\partial\alpha_{\rm s}(Q^2x)}{\partial\ln x} = -\frac{\beta_0}{4\pi}\left[\alpha_{\rm s}(Q^2x)\right]^2 - \frac{\beta_1}{8\pi^2}\left[\alpha_{\rm s}(Q^2x)\right]^3. \tag{3.1}$$

The solution of (3.1), obtained by keeping the leading $(\alpha_{\rm s}\ln x)^k$ and next-to-leading $\alpha_{\rm s}(\alpha_{\rm s}\ln x)^{k-1}$ powers of $\ln x$, reads [50]

$$\alpha_{\rm s}(Q^2x) \simeq \frac{\alpha_{\rm s}(Q^2)}{1+\ln x/t}\left[1 - \frac{\alpha_{\rm s}(Q^2)\beta_1}{2\pi\beta_0}\frac{\ln[1+\ln x/t]}{1+\ln x/t}\right], \tag{3.2}$$

where $\alpha_{\rm s}(Q^2)$ is the one-loop QCD coupling constant and $t = 4\pi/\beta_0\alpha_{\rm s}(Q^2)$.

Inserting (3.2) into the expressions for the hard-scattering amplitudes and subsequently $T_{1,2}^{q(g)}(x,Q^2,\omega)$ into (2.14) and (2.15), we obtain integrals which are still divergent, but which now can be calculated using existing methods. One of these methods, applied in [30] for the calculation of the electromagnetic pion form factor, allows us to find the quantity under consideration as a perturbative series in $\alpha_{\rm s}(Q^2)$ with factorially growing coefficients $C_n \sim (n-1)!$. Similar series with coefficients $C_n \sim (n-1)!$ may be found also for the form factor $Q^2F_{\eta' g^* g^*}(Q^2,\omega)$, i.e.,

$$Q^2F_{\eta' g^* g^*}(Q^2,\omega) \sim \sum_{n=1}^{\infty}\left[\frac{\alpha_{\rm s}(Q^2)}{4\pi}\right]^n \beta_0^{n-1}C_n. \tag{3.3}$$

But a perturbative QCD series with factorially growing coefficients is a signal for the IR renormalon nature of the divergences in (3.3). The convergence radius of the series (3.3) is zero and its resummation should be performed by employing the Borel integral technique. First, one has to find the Borel transform $B[Q^2F_{\eta' g^* g^*}](u)$ of the corresponding series [51],

$$B\left[Q^2F_{\eta' g^* g^*}\right](u) = \sum_{n=1}^{\infty}\frac{u^{n-1}}{(n-1)!}C_n. \tag{3.4}$$

Because the coefficients of the series (3.3) behave like $C_n \sim (n-1)!$, the Borel transform (3.4) contains poles located at the positive u axis of the Borel plane. In other words, the divergence of the series (3.3) owing to (3.4) has been transformed into pole-like singularities of the function $B[Q^2F_{\eta' g^* g^*}](u)$. These poles are the footprints of the IR renormalons.

Now in order to define the sum (3.3) or to find the resummed expression for the form factor, one has to invert $B[Q^2F_{\eta' g^* g^*}](u)$ to get

$$\left[Q^2F_{\eta' g^* g^*}(Q^2,\omega)\right]^{\rm res} \sim {\rm P.V.}\int_0^{\infty}{\rm d}u\exp\left[-\frac{4\pi}{\beta_0\alpha_{\rm s}(Q^2)}u\right]B\left[Q^2F_{\eta' g^* g^*}\right](u) \tag{3.5}$$

and remove the IR renormalon divergences by the principal value prescription.

The procedure described above is straightforward but, at the same time, tedious. Fortunately, these intermediate operations can be bypassed by introducing the inverse Laplace transforms of the functions in (3.2) [52], viz.,

$$\frac{1}{(t+z)^{\nu}} = \frac{1}{\Gamma(\nu)}\int_0^{\infty}{\rm d}u\exp[-u(t+z)]u^{\nu-1}, \quad {\rm Re}\nu > 0 \tag{3.6}$$

and

$$\frac{\ln(t+z)}{(t+z)^2} = \int_0^{\infty}{\rm d}u\exp[-u(t+z)](1-\gamma_{\rm E}-\ln u)u, \tag{3.7}$$

where $\Gamma(z)$ is the Gamma function, $\gamma_{\rm E} \simeq 0.577216$ is the Euler constant, and $z = \ln x$ [or $z = \ln\overline{x}$].

Then using (3.2), (3.6) and (3.7) for $\alpha_{\rm s}(Q^2x)$, we get [6]

$$\alpha_{\rm s}(Q^2x) = \alpha_{\rm s}(Q^2)t\int_0^{\infty}{\rm d}u\exp(-ut)x^{-u}R(u,t) = \frac{4\pi}{\beta_0}\int_0^{\infty}{\rm d}u\exp(-ut)x^{-u}R(u,t), \tag{3.8}$$

with the function $R(u,t)$ defined as

$$R(u,t) = 1 - \frac{2\beta_1}{\beta_0^2}u(1-\gamma_{\rm E}-\ln t-\ln u). \tag{3.9}$$

Employing (3.8) for $\alpha_{\rm s}(Q^2x)$ and carrying out the integrations over x, we obtain (see the next section) the quark and gluon components of the form factor $F_{\eta' g^* g^*}(Q^2,\omega)$ directly in the Borel resummed form (3.5).

The resummed vertex function $[Q^2 F_{\eta' g^* g^*}(Q^2,\omega)]^{\rm res}$ – except for the η'-meson–on-shell-gluon transition and the $\omega = 0$ case – contains an infinite number of IR renormalon poles located at $u_0 = n$, where n is a positive integer that, in general, is given as a sum of a series, i.e.,

$$S(k_0, Q^2, \omega) \sim \sum_{n=k_0}^{\infty} \frac{4\pi}{\beta_0} \mathrm{P.V.} \int_0^{\infty} \frac{\mathrm{e}^{-ut} R(u,t) \mathrm{d}u}{n-u} C_n(\omega). \tag{3.10}$$

One appreciates that all information on the process asymmetry parameter ω is accumulated in the coefficient functions $C_n(\omega)$.

To avoid inessential technical details and to make the presentation as transparent as possible, let us for the time being neglect the non-leading term $\sim \alpha_{\rm s}^2$ in (3.2) and make the replacement $R(u,t) \to 1$ in (3.10). Then, the integrals in (3.10) take, after simple manipulations, the form

$$\frac{4\pi}{\beta_0} \mathrm{P.V.} \int_0^{\infty} \frac{\mathrm{e}^{-ut} \mathrm{d}u}{n-u} = \frac{4\pi}{\beta_0} \frac{\mathrm{li}(\lambda^n)}{\lambda^n}, \quad \lambda = Q^2/\Lambda^2, \tag{3.11}$$

with the logarithmic integral $\mathrm{li}(\xi)$ defined by

$$\mathrm{li}(\xi) = \mathrm{P.V.} \int_0^{\xi} \frac{\mathrm{d}t}{\ln t}. \tag{3.12}$$

The function $\mathrm{li}(\xi)$ is expressible in terms of the function $E_1(z)$ [49]

$$\mathrm{li}(\xi) = -E_1(-\ln \xi), \tag{3.13}$$

where

$$E_1(z) = \int_z^{\infty} \mathrm{e}^{-t} t^{-1} \mathrm{d}t.$$

The latter expression can, for $|z| \to \infty$, be expanded over inverse powers of z

$$E_1(z) = z^{-1} \mathrm{e}^{-z} \left[\sum_{m=0}^{M} \frac{m!}{(-z)^m} + O\left(|z|^{-(M+1)} \right) \right]. \tag{3.14}$$

Using (3.13) and (3.14), we find

$$\mathrm{li}(\xi) \simeq \frac{\xi}{\ln \xi} \sum_{m=0}^{M} \frac{m!}{(\ln \xi)^m}, \qquad \frac{\mathrm{li}(\xi^n)}{\xi^n} \simeq \frac{1}{n \ln \xi} \sum_{m=0}^{M} \frac{m!}{(n \ln \xi)^m}. \tag{3.15}$$

It is not difficult to see that for $Q^2 \gg \Lambda^2$

$$\frac{4\pi}{\beta_0} \frac{\mathrm{li}(\lambda^n)}{\lambda^n} \simeq 4\pi \sum_{m=1}^{M} \left[\frac{\alpha_{\rm s}(Q^2)}{4\pi} \right]^m \beta_0^{m-1} \frac{(m-1)!}{n^m}. \tag{3.16}$$

Choosing in (3.16) $M \to \infty$ and comparing the obtained result with (3.3), we conclude that each term in the sum (3.10) at fixed n is the resummed Borel expression of the series (3.16).

But we can look at the integrals in (3.10) from another perspective. Namely, it is easy to show that

$$\frac{4\pi}{\beta_0} \int_0^{\infty} \frac{\mathrm{e}^{-ut} \mathrm{d}u}{n-u} = \int_0^1 \alpha_{\rm s}(Q^2 x) x^{n-1} \mathrm{d}x = \frac{1}{n} f_{2n}(Q), \tag{3.17}$$

where $f_{2n}(Q)$ are the moment integrals

$$f_p(Q) = \frac{p}{Q^p} \int_0^Q \mathrm{d}k k^{p-1} \alpha_{\rm s}(k^2). \tag{3.18}$$

The integrals $f_p(Q)$ can be calculated using the IR matching scheme [53]

$$f_p(Q) = \left(\frac{\mu_I}{Q} \right)^p f_p(\mu_I) + \alpha_{\rm s}(Q^2) \sum_{n=0}^{N} \left[\frac{\beta_0}{2\pi p} \alpha_{\rm s}(Q^2) \right]^n \times \left[n! - \Gamma\left(n+1, \quad p \ln(Q/\mu_I)\right) \right], \tag{3.19}$$

where μ_I is the infrared matching scale and $\Gamma(n+1,z)$ is the incomplete Gamma function

$$\Gamma\left(n+1,\, z\right) = \int_z^{\infty} \mathrm{e}^{-t} t^n \mathrm{d}t. \tag{3.20}$$

In (3.19) $f_p(\mu_I)$ are phenomenological parameters, which represent the weighted average of $\alpha_{\rm s}(k^2)$ over the IR region $0 < k < \mu_I$ and act at the same time as infrared regulators of the RHS of (3.17). The first term on the RHS of (3.19) is a power-suppressed contribution to $f_p(Q)$, which cannot be calculated within pQCD, whereas the second term is the perturbatively calculable part of the function $f_p(Q)$. Stated differently, the infrared matching scheme allows one to estimate power corrections to the moment integrals by explicitly dissecting them from the full expression and introducing new non-perturbative parameters $f_p(\mu_I)$. The values of these parameters have to be extracted from experimental data.

In order to check the accuracy of both the RC method (IR renormalon calculus) and the infrared matching scheme, a Landau-pole free model for $\alpha_{\rm s}(Q^2)$ was introduced in [53] yielding

$$\alpha_{\rm s}(Q^2) = \frac{4\pi}{\beta_0} \left[\frac{1}{\ln \lambda} + 125 \frac{1+4\lambda}{(1-\lambda)(4+\lambda)^4} \right]. \tag{3.21}$$

The model expression (3.21) was used for the exact calculation of the moment integrals $f_p^{\rm exact}(Q)$. The IR renormalon and the IR matching scheme results were compared with $f_p^{\rm exact}(Q)$ concluding that for $N \geq 2$ the IR matching scheme leads to a good agreement with the exact values of $f_p(Q)$. As regards the calculation of the integrals $f_p(Q)$, when employing the RC method with the principal value prescription, a good agreement with $f_2^{\rm exact}(Q)$ was found for $p = 2$, while for $p = 1$ a small deviation from $f_1^{\rm exact}(Q)$ in the region of $Q^2 \sim$ a few GeV^2 was observed (the lowest moment integral entering into our expressions is $f_2(Q)$). But even for $p = 1$, the agreement with $f_1^{\rm exact}(Q)$ within the error bars is quite satisfactory in view of the uncertainties produced by the principal value prescription itself. Therefore, we can conclude that the RC method and the IR matching scheme lead for the moment integrals $f_p(Q)$ to approximately similar numerical results. It is remarkable

that in both cases an enhancement of the IR renormalon and matching scheme results relative to the leading-order perturbative prediction was found.

After presenting our analysis, it becomes evident that the Borel resummation technique enables us to estimate with a rather good accuracy power-behaved corrections to the integrals in (3.10) and hence to the vertex function $F_{\eta' g^* g^*}(Q^2,\omega)$. Of course, one can employ the IR matching scheme and (3.19) to determine power corrections to the form factor in explicit form. But as we have noted above, in general, the form factor $Q^2 F_{\eta' g^* g^*}(Q^2,\omega)$ contains an infinite number of IR renormalon poles, or, stated equivalently, an infinite number of $f_{2n}(Q)$ is required to calculate sums like the one presented in (3.10). In real numerical computations, in order to reach a good approximation of the series (3.10), at least a sum of the first $15 \div 20$ terms is needed, meaning the involvement of $f_{2n}(\mu_I)$ $(n = 15 \div 20)$ non-perturbative parameters. But from the experimental data, only the first few moments $f_p(\mu_I)$ could be extracted [54–57]. Values for $f_1(2\,\mathrm{GeV})$ (in the literature the notation $f_1(\mu_I) = \alpha_0(\mu_I)$ is widely used) range from $\alpha_0(2\,\mathrm{GeV}) = 0.435 \pm 0.021$ [54] and $\alpha_0(2\ \mathrm{GeV}) = 0.513^{+0.066}_{-0.045}$ [55] to $\alpha_0(2\,\mathrm{GeV}) = 0.597^{+0.009}_{-0.010}$ [56]. Here, we write down only sample results, obtained in these works, in order to demonstrate the experimental situation with $\alpha_0(2\,\mathrm{GeV}) = f_1(2\,\mathrm{GeV})$. For $f_2(2\,\mathrm{GeV})$ the value $f_2(2\,\mathrm{GeV}) \simeq 0.5$ was deduced [53, 58] from the data on structure functions [57].

In the framework of the RC method, we estimate the same power corrections to a physical quantity, but here we do not need additional information on $f_p(\mu_I)$. Moreover, this method gives us the possibility to calculate values of the non-perturbative parameters $f_p(\mu_I)$ by means of the formula

$$f_{2n}(\mu_I) = n\frac{4\pi}{\beta_0}\frac{\mathrm{li}\left(\widetilde{\lambda}^n\right)}{\widetilde{\lambda}^n}, \quad \widetilde{\lambda} = \mu_I^2/\Lambda^2, \tag{3.22}$$

which can easily be found by comparing (3.11) and (3.17). The calculated values of the first few even moments ($n_f = 3,\ \Lambda = 0.3\,\mathrm{GeV}$) are

$$\begin{aligned} &f_2(2\,\mathrm{GeV}) \simeq 0.535, \quad f_4(2\,\mathrm{GeV}) \simeq 0.45, \\ &f_6(2\,\mathrm{GeV}) \simeq 0.41. \end{aligned} \tag{3.23}$$

To compare our predictions with those computed via the model $\alpha_{\mathrm{s}}(Q^2)$ (see (3.21)), we choose $n_f = 3$ and $\Lambda = 0.25\,\mathrm{GeV}$. The corresponding values are shown below:

$$\begin{aligned} f_2^{\mathrm{RC}}(2\,\mathrm{GeV}) \simeq 0.479, \quad f_4^{\mathrm{RC}}(2\,\mathrm{GeV}) \simeq 0.393, \\ f_2^{\mathrm{mod}}(2\,\mathrm{GeV}) \simeq 0.450, \quad f_4^{\mathrm{mod}}(2\,\mathrm{GeV}) \simeq 0.388. \end{aligned} \tag{3.24}$$

One observes that the parameters $f_p(\mu_I)$ of the RC method are in agreement with both the experimental results and the model calculations.

We have noted above that the principal value prescription, adopted in this work in order to regularize divergent integrals (see (3.5) and (3.10)) generates power-suppressed (higher-twist) uncertainties

$$\sim \sum_q N_q \frac{\Phi_q(Q^2)}{Q^{2q}}, \tag{3.25}$$

where $\{\Phi_q(Q^2)\}$ are calculable functions entirely fixed by the residues of the Borel transform $B[Q^2 F_{Mg^* g^*}](u)$ at the poles $q = u_0$ and $\{N_q\}$ are arbitrary constants to be fixed from the experimental data. In the case of the $\eta'\gamma$ electromagnetic transition form factor $Q^2 F_{\eta'\gamma}(Q^2)$, the uncertainties (3.25) were estimated in [6]. For the η'-meson asymptotic DA and for the parameters $N_1 = N_2 = 1$ and $N_1 = N_2 = -1$, it was found that they do not exceed $\pm 15\%$ of the $\eta'\gamma$ form factor. Because the RC method allows one to evaluate power corrections to a physical quantity, in general, and for the $\eta'\gamma$ transition form factor it has already provided a good agreement with the CLEO data [6], one has to introduce the constraint $|N_{1,2}| \ll 1$ in order to retain this agreement. In the present work we shall estimate in our numerical analysis the higher-twist uncertainties produced by the principal value prescription by choosing the constants $\{N_q\} = \pm 1$. It will be demonstrated that the $\pm 15\%$ bounds are valid also for the $\eta' g,\ \eta' g^*$ transition FFs. Inclusion of higher-twist corrections, arising from the two-particle higher-twist and higher Fock states DAs of the η' meson, may, in principle, further improve this scheme. These refinements are, however, beyond the scope of the present investigation.

4 The form factor $F_{\eta' g^* g^*}(Q^2,\omega)$ within the RC method

In this section we calculate the quark and gluon components of the vertex function $F_{\eta' g^* g^*}(Q^2,\omega)$ within the RC method. We also present our results for $F_{\eta' g g^*}(Q^2, \omega = \pm 1)$, $F_{\eta' g^* g^*}(Q^2, \omega = 0)$ and the asymptotic limit for the form factor.

4.1 Quark component $F^q_{\eta' g^* g^*}(Q^2,\omega)$ of the vertex function

To calculate the quark component of the vertex function $F^q_{\eta' g^* g^*}(Q^2,\omega)$, we use (2.25) for $F^q_{\eta' g^* g^*}(Q^2,\omega)$, (2.29) for the hard-scattering amplitude $T_1^q(x,Q^2,\omega)$, and the expression for $\alpha_{\mathrm{s}}(Q^2 x)$ given in (3.8). Employing the quark component of the η'-meson DA, $\phi^q(x,Q^2)$, we get[4]

$$\begin{aligned} &Q^2 F^q_{\eta' g^* g^*}(Q^2,\omega) \\ &= -\frac{32\pi^2 C[1+A(Q^2)]}{\beta_0}\int_0^\infty \mathrm{d}u \mathrm{e}^{-ut} R(u,t) \\ &\quad \times \left[\int_0^1 \frac{x^{1-u}\overline{x}\mathrm{d}x}{(1+\omega)x + (1-\omega)\overline{x}}\right. \end{aligned}$$

[4] In what follows integrals over the variable u have to be understood in the sense of the Cauchy principal value

$$+\int_0^1 \frac{x\overline{x}^{1-u}\mathrm{d}x}{(1+\omega)x+(1-\omega)\overline{x}}\Bigg]$$
$$+\frac{160\pi^2 CA(Q^2)}{\beta_0}\int_0^\infty \mathrm{d}u e^{-ut}R(u,t)$$
$$\times\left[\int_0^1 \frac{x^{2-u}\overline{x}^2\mathrm{d}x}{(1+\omega)x+(1-\omega)\overline{x}}\right.$$
$$\left.+\int_0^1 \frac{x^2\overline{x}^{2-u}\mathrm{d}x}{(1+\omega)x+(1-\omega)\overline{x}}\right]. \quad (4.1)$$

Using the fact that the integral [59]

$$\int_0^1 x^{\alpha-1}\overline{x}^{\beta-1}(1-xr)^\gamma \mathrm{d}x = B(\alpha,\beta)\,{}_2F_1\left(-\gamma,\alpha;\alpha+\beta;r\right) \quad (4.2)$$

is expressible in terms of the Gauss hypergeometric function [60]

$${}_2F_1(a,b;c;z)=\sum_{k=0}^{\infty}\frac{(a)_k(b)_k}{(c)_k}\frac{z^k}{k!}, \quad (4.3)$$

we obtain

$$Q^2F^q_{\eta' g^* g^*}(Q^2,\omega)$$
$$=-\frac{32\pi^2C[1+A(Q^2)]}{\beta_0(1+\omega)}\int_0^\infty \mathrm{d}u e^{-ut}R(u,t)B(2-u,2)$$
$$\times\left[{}_2F_1\left(1,2;4-u;\frac{2\omega}{1+\omega}\right)\right.$$
$$\left.+\,{}_2F_1\left(1,2-u;4-u;\frac{2\omega}{1+\omega}\right)\right]$$
$$+\frac{160\pi^2CA(Q^2)}{\beta_0(1+\omega)}\int_0^\infty \mathrm{d}u e^{-ut}R(u,t)B(3-u,3)$$
$$\times\left[{}_2F_1\left(1,3;6-u;\frac{2\omega}{1+\omega}\right)\right.$$
$$\left.+{}_2F_1\left(1,3-u;6-u;\frac{2\omega}{1+\omega}\right)\right]. \quad (4.4)$$

In (4.2) and (4.3), $B(x,y)$ and $(a)_n$ are the Beta function and Pochhammer symbols, respectively, defined in terms of the Gamma function $\Gamma(z)$:

$$B(x,y)=\frac{\Gamma(x)\Gamma(y)}{\Gamma(x+y)},\quad (a)_n=\frac{\Gamma(a+n)}{\Gamma(a)}.$$

From (4.4) a simple expression for the η'-meson–on-shell-gluon transition form factor $F^q_{\eta' g g^*}(Q^2,\omega=\pm1)$ can be found:

$$Q^2F^q_{\eta' g g^*}(Q^2,\omega=\pm1)=-\frac{16\pi^2C[1+A(Q^2)]}{\beta_0}$$
$$\times\int_0^\infty \mathrm{d}u e^{-ut}R(u,t)\left[B(1,2-u)+B(2,1-u)\right]$$
$$+\frac{80\pi^2CA(Q^2)}{\beta_0}\int_0^\infty \mathrm{d}u e^{-ut}R(u,t)$$
$$\times\left[B(3,2-u)+B(2,3-u)\right], \quad (4.5)$$

where we have used the equality [60]

$${}_2F_1(a,b;c;1)=\frac{\Gamma(c)\Gamma(c-a-b)}{\Gamma(c-a)\Gamma(c-b)}. \quad (4.6)$$

It is worth noting that (4.5) can be obtained from (2.25) by employing the $\omega\to\pm1$ limits of the hard-scattering amplitudes (2.29):

$$T_1^q(x,Q^2,\omega=\pm1)+T_2^q(x,Q^2,\omega=\pm1)$$
$$=-\frac{\pi}{3Q^2}\left[\alpha_{\rm s}(Q^2x)+\alpha_{\rm s}(Q^2\overline{x})\right]\left[\frac{1}{x}+\frac{1}{\overline{x}}\right]. \quad (4.7)$$

In the case of gluons with equal virtualities $Q_1^2=Q_2^2$ (and hence in the $\omega=0$ case), the form factor can be found employing the expression for the hard-scattering amplitude

$$T_1^q(x,Q^2,\omega=0)+T_2^q(x,Q^2,\omega=0)$$
$$=-\frac{4\pi}{3Q^2}\left[\alpha_{\rm s}(Q^2x)+\alpha_{\rm s}(Q^2\overline{x})\right]. \quad (4.8)$$

Calculation leads to the simple expression

$$Q^2F^q_{\eta' g^* g^*}(Q^2,\omega=0)$$
$$=-\frac{64\pi^2C(1+A(Q^2))}{\beta_0}\int_0^\infty \mathrm{d}u e^{-ut}R(u,t)B(2-u,2)$$
$$+\frac{320\pi^2CA(Q^2)}{\beta_0}\int_0^\infty \mathrm{d}u e^{-ut}R(u,t)B(3-u,3). \quad (4.9)$$

Let us note that (4.9) can be deduced from (4.4) in the limit $\omega\to0$ by taking into account that [60]

$${}_2F_1(a,b;c;0)=1.$$

The next important problem to be solved within the framework of the RC method, is to reveal the IR renormalon poles in (4.4), (4.5) and (4.9) because without such a clarification all these expressions would have merely a formal character.

We start from the simple case, i.e., from (4.5), and get

$$B(1,2-u)+B(2,1-u)$$
$$=\frac{\Gamma(1)\Gamma(2-u)}{\Gamma(3-u)}+\frac{\Gamma(2)\Gamma(1-u)}{\Gamma(3-u)}$$
$$=\frac{1}{2-u}+\frac{1}{(1-u)(2-u)}=\frac{1}{1-u}$$

and

$$B(3,2-u)+B(2,3-u)$$
$$=\frac{\Gamma(3)\Gamma(2-u)}{\Gamma(5-u)}+\frac{\Gamma(2)\Gamma(3-u)}{\Gamma(5-u)}$$
$$=\frac{2}{(2-u)(3-u)(4-u)}+\frac{1}{(3-u)(4-u)}$$
$$=\frac{1}{2-u}-\frac{1}{3-u}.$$

In deriving these expressions we used the following property of the Gamma function:

$$z\Gamma(z) = \Gamma(z+1).$$

Hence we have

$$\begin{aligned} &Q^2 F^q_{\eta' gg^*}(Q^2, \omega = \pm 1) \qquad (4.10)\\ &= -\frac{16\pi^2 C[1+A(Q^2)]}{\beta_0}\int_0^\infty \mathrm{e}^{-ut} R(u,t)\frac{\mathrm{d}u}{1-u}\\ &+ \frac{80\pi^2 C A(Q^2)}{\beta_0}\int_0^\infty \mathrm{e}^{-ut} R(u,t)\left(\frac{1}{2-u}-\frac{1}{3-u}\right)\mathrm{d}u. \end{aligned}$$

As one sees, the structure of the IR renormalon poles is very simple; we encounter only a finite number of single poles located at $u_0 = 1$, 2 and 3.

In the same manner we get from (4.9)

$$\begin{aligned} &Q^2 F^q_{\eta' g^* g^*}(Q^2, \omega = 0)\\ &= -\frac{64\pi^2 C(1+A(Q^2))}{\beta_0}\\ &\qquad \times \int_0^\infty \mathrm{d}u \mathrm{e}^{-ut} R(u,t)\frac{1}{(2-u)(3-u)}\\ &+ \frac{640\pi^2 C A(Q^2)}{\beta_0} \qquad (4.11)\\ &\qquad \times \int_0^\infty \mathrm{d}u \mathrm{e}^{-ut} R(u,t)\frac{1}{(3-u)(4-u)(5-u)}. \end{aligned}$$

In this case the single IR renormalon poles are located at the points $u_0 = 2,\ 3,\ 4$ and 5.

In order to get the IR renormalon structure of the integrands in (4.4), we have to expand the hypergeometric function ${}_2F_1(a,b;c;z)$ in powers of z (see (4.3)), where the condition $|z| < 1$ must hold. But the argument of the function ${}_2F_1(a,b;c;2\omega/(1+\omega))$ satisfies this requirement only in the region $\omega \in (0,1)$. In the region $\omega \in (-1,0)$ an expression obtained from (4.4) by means of a simple transformation (see (4.17) below) has to be used because in this case the argument of the hypergeometric function becomes equal to $2\omega/(\omega-1) < 1$, obeying in the region $\omega \in (-1,0)$ the required constraint. But regardless of the expansion region, we obtain in both cases the same IR renormalon structure. Adding to this argumentation the evident fact that the vertex function is symmetric under the replacement $\omega \leftrightarrow -\omega$ (cf. (2.27)), we can restrict the study of the form factor $Q^2 F^q_{\eta' g^* g^*}(Q^2,\omega)$ to the region $\omega \in (0,1)$. Then, we can expand the hypergeometric functions ${}_2F_1(a,b;c;2\omega/(1+\omega))$ in the region $\omega \in (0,1)$, via (4.3). For example, for one of these functions, we get

$$\begin{aligned} &B(2,2-u)_2F_1\,(1,2;4-u;\beta)\\ &= \frac{\Gamma(2)\Gamma(2-u)}{\Gamma(4-u)}\sum_{k=0}^\infty \frac{(1)_k (2)_k}{(4-u)_k}\frac{\beta^k}{k!}\\ &= \sum_{k=0}^\infty \frac{\Gamma(k+2)\Gamma(2-u)}{\Gamma(k+4-u)}\beta^k = \sum_{k=0}^\infty B(k+2,2-u)\beta^k, \end{aligned}$$

with

$$\beta = \frac{2\omega}{1+\omega}.$$

The remaining terms in (4.4) can be treated in the same manner and as a result we obtain

$$\begin{aligned} &Q^2 F^q_{\eta' g^* g^*}(Q^2,\omega)\\ &= -\frac{32\pi^2 C[1+A(Q^2)]}{\beta_0(1+\omega)}\int_0^\infty \mathrm{d}u \mathrm{e}^{-ut} R(u,t)\\ &\qquad \times \sum_{k=0}^\infty \left[B(2-u,k+2)+B(2,k+2-u)\right]\beta^k\\ &+ \frac{160\pi^2 C A(Q^2)}{\beta_0(1+\omega)}\int_0^\infty \mathrm{d}u \mathrm{e}^{-ut} R(u,t) \qquad (4.12)\\ &\qquad \times \sum_{k=0}^\infty \left[B(3-u,k+3)+B(3,k+3-u)\right]\beta^k. \end{aligned}$$

The IR renormalon structure of the integrands in (4.12) is quite clear now. In fact, we can write the Beta functions entering (4.12) in the following form:

$$\begin{aligned} B(2,k+2-u) &= \frac{\Gamma(2)\Gamma(k+2-u)}{\Gamma(k+4-u)}\\ &= \frac{1}{(k+2-u)(k+3-u)} \end{aligned}$$

and correspondingly

$$\begin{aligned} B(2-u,k+2) &= \frac{\Gamma(k+2)}{(2-u)(3-u)\ldots(k+3-u)},\\ B(3,k+3-u) &= \frac{2}{(k+3-u)(k+4-u)(k+5-u)},\\ B(3-u,k+3) &= \frac{\Gamma(k+3)}{(3-u)(4-u)\ldots(k+5-u)}. \end{aligned}$$

Here we have an infinite number of single IR renormalon poles located at the points $u_0 = k+2,\ k+3;\ u_0 = 2,\ 3, \ldots k+3;\ u_0 = k+3,\ k+4,\ k+5$ and $u_0 = 3,\ 4, \ldots, k+5$, respectively.

The last question to be answered is whether one can use our results, obtained in the context of the RC method, in the limit $Q^2 \to \infty$ in order to regain the asymptotic form of the form factor $F^q_{\eta' g^* g^*}(Q^2 \to \infty, \omega)$. It is clear that regardless of the methods employed and the approximations done, in the limit $Q^2 \to \infty$ the form factor $F^q_{\eta' g^* g^*}(Q^2,\omega)$ must reach its asymptotic form. This is true, of course, for our computations, as we estimate power-suppressed corrections to the form factor $Q^2 F^q_{\eta' g^* g^*}(Q^2,\omega)$, which become important in a region of $Q^2 \sim$ of a few GeV^2, but vanish in the asymptotic limit. As we have emphasized in Sect. 2, in the asymptotic limit the gluon DA of the η'-meson satisfies $\phi^g(x,Q^2) \to 0$ and hence

$$Q^2 F^g_{\eta' g^* g^*}(Q^2,\omega) \overset{Q^2\to\infty}{\longrightarrow} 0.$$

The DA of the quark component $\phi^q(x,Q^2)$ of the η' meson evolves for $Q^2 \to \infty$ to the asymptotic DA (2.37) and all non-asymptotic terms in $\phi^q(x,Q^2)$ proportional to $C_n^{3/2}(x-\overline{x})$, $n>0$ (in our case $\sim A(Q^2)$) vanish. Therefore, the results which we shall obtain here describe not only the asymptotic limit of $Q^2 F^q_{\eta' g^* g^*}(Q^2,\omega)$, but also the asymptotic limit of the vertex function $Q^2 F_{\eta' g^* g^*}(Q^2,\omega)$ itself.

In the limit $Q^2 \to \infty$ the asymmetry parameter can take values $\omega \to \pm 1$ (if we pass to the limit $Q^2 \to \infty$ at fixed Q_2^2 or Q_1^2), $\omega = 0$ ($Q_1^2 = Q_2^2$ and $Q^2 \to \infty$) or $\omega \neq \pm 1,\ 0$ (if we take the limit $Q^2 \to \infty$ at fixed ω). We consider here all possibilities:
(a) $Q^2 \to \infty,\ \omega \to \pm 1$,
(b) $Q^2 \to \infty,\ \omega = 0$ and
(c) $Q^2 \to \infty,\ \omega \neq \pm 1,\ 0$.

In the limit $Q^2 \to \infty$, we also take into account that the second term in the expansion $\alpha_{\rm s}(Q^2 x)$ (3.8) has to be neglected. In other words, in the limit $Q^2 \to \infty$, we find

$$\int_0^\infty \mathrm{e}^{-ut} R(u,t)\mathrm{d}u \to \int_0^\infty \mathrm{e}^{-ut}\mathrm{d}u. \tag{4.13}$$

We begin from the simpler case (a). In (4.10) we have already obtained the desired limit, but $A(Q^2) \neq 0$. Taking into account (4.13) and $A(Q^2) \to 0$, we get

$$Q^2 F_{\eta' g g^*}(Q^2, \omega = \pm 1) \overset{Q^2\to\infty}{\longrightarrow} -\frac{16\pi^2 C}{\beta_0}\int_0^\infty \frac{\mathrm{e}^{-ut}\mathrm{d}u}{1-u} = -\frac{16\pi^2 C}{\beta_0}\frac{\mathrm{li}(\lambda)}{\lambda}.$$

It is easy to show that using only the leading term in the expansion of $\mathrm{li}(\lambda)/\lambda$ (see (3.15)), we find

$$Q^2 F_{\eta' g g^*}(Q^2, \omega = \pm 1) \overset{Q^2\to\infty}{\longrightarrow} -4\pi C \alpha_{\rm s}(Q^2). \tag{4.14}$$

The limit $Q^2 \to \infty,\ \omega = 0$ can be analyzed by similar means. Thus, from (4.11) we get

$$Q^2 F_{\eta' g^* g^*}(Q^2, \omega = 0) \overset{Q^2\to\infty}{\longrightarrow} -\frac{64\pi^2 C}{\beta_0}\int_0^\infty \frac{\mathrm{e}^{-ut}\mathrm{d}u}{(2-u)(3-u)} = -\frac{64\pi^2 C}{\beta_0}\left[\frac{\mathrm{li}(\lambda^2)}{\lambda^2} - \frac{\mathrm{li}(\lambda^3)}{\lambda^3}\right],$$

which in the limit under consideration simplifies to

$$Q^2 F_{\eta' g^* g^*}(Q^2, \omega = 0) \overset{Q^2\to\infty}{\longrightarrow} -\frac{8\pi C \alpha_{\rm s}(Q^2)}{3}. \tag{4.15}$$

Now let us consider the more interesting case (c). Then, from (4.4) and (4.13), we obtain

$$Q^2 F_{\eta' g^* g^*}(Q^2,\omega) \overset{Q^2\to\infty}{\longrightarrow} -\frac{32\pi^2 C}{\beta_0(1+\omega)}\int_0^\infty \mathrm{d}u \mathrm{e}^{-ut} B(2,2-u) \times \left[{}_2F_1\left(1,2;4-u;\frac{2\omega}{1+\omega}\right) + {}_2F_1\left(1,2-u;4-u;\frac{2\omega}{1+\omega}\right)\right]. \tag{4.16}$$

As an example, we analyze the second term in (4.16) (see also (4.12))

$$\begin{aligned}
&\int_0^\infty \mathrm{d}u \mathrm{e}^{-ut} B(2,2-u)\,{}_2F_1\left(1,2-u;4-u;\beta\right)\\
&= \int_0^\infty \mathrm{d}u \mathrm{e}^{-ut}\sum_{k=0}^\infty B(2,k+2-u)\beta^k\\
&= \sum_{k=0}^\infty \Gamma(2)\beta^k \int_0^\infty \mathrm{d}u \mathrm{e}^{-ut}\left(\frac{1}{k+2-u} - \frac{1}{k+3-u}\right)\\
&= \sum_{k=0}^\infty \Gamma(2)\left[\frac{\mathrm{li}(\lambda^{k+2})}{\lambda^{k+2}} - \frac{\mathrm{li}(\lambda^{k+3})}{\lambda^{k+3}}\right]\beta^k.
\end{aligned}$$

In the considered limit, one finds

$$\frac{\mathrm{li}(\lambda^{k+2})}{\lambda^{k+2}} - \frac{\mathrm{li}(\lambda^{k+3})}{\lambda^{k+3}} \to \frac{1}{\ln\lambda}\left(\frac{1}{k+2} - \frac{1}{k+3}\right) = \frac{1}{\ln\lambda}\frac{1}{(k+2)(k+3)}.$$

Then, the result reads

$$\begin{aligned}
&\sum_{k=0}^\infty \Gamma(2)\left[\frac{\mathrm{li}(\lambda^{k+2})}{\lambda^{k+2}} - \frac{\mathrm{li}(\lambda^{k+3})}{\lambda^{k+3}}\right]\beta^k \to\\
&\frac{1}{\ln\lambda}\sum_{k=0}^\infty \frac{\Gamma(2)}{(k+2)(k+3)}\beta^k\\
&= \frac{1}{\ln\lambda}\sum_{k=0}^\infty B(2,k+2)\beta^k = \frac{1}{\ln\lambda}B(2,2)\,{}_2F_1(1,2;4;\beta).
\end{aligned}$$

The same method can be applied to the first function in (4.16). But before doing that, it is instructive to employ the transformation

$${}_2F_1(a,b,c;z) = (1-z)^{-a}\,{}_2F_1\left(a,c-b,c;\frac{z}{z-1}\right). \tag{4.17}$$

After performing all these operations we find

$$\begin{aligned}
&Q^2 F_{\eta' g^* g^*}(Q^2,\omega) \overset{Q^2\to\infty}{\longrightarrow}\\
&-\frac{64\pi^2 C}{\beta_0(1+\omega)}\frac{1}{\ln\lambda}B(2,2)\,{}_2F_1(1,2;4;\beta)\\
&= -\frac{8\pi C\alpha_{\rm s}(Q^2)}{3(1+\omega)}\,{}_2F_1(1,2;4;\beta).
\end{aligned} \tag{4.18}$$

Taking into account the expression for the hypergeometric function ${}_2F_1(1,2;4;\beta)$ in terms of elementary ones [60],

$${}_2F_1(1,2;4;\beta) = \frac{3}{\beta^3}\left[\beta(2-\beta) + 2(1-\beta)\ln(1-\beta)\right], \tag{4.19}$$

we finally obtain

$$Q^2 F_{\eta' g^* g^*}(Q^2,\omega) \overset{Q^2\to\infty}{\longrightarrow} -4\pi C\alpha_{\rm s}(Q^2) f(\omega),$$
$$f(\omega) = \frac{1}{\omega^2}\left(1+\frac{1-\omega^2}{2\omega}\ln\frac{1-\omega}{1+\omega}\right). \tag{4.20}$$

In our argumentations we have tacitly assumed that $\omega \in (0,1)$. But (4.20) holds for all values of $\omega \neq \pm 1,\ 0$, which is evident from the equality $f(\omega) = f(-\omega)$.

Equations (4.14), (4.15) and (4.20) can be obtained in the standard HSA using the corresponding hard-scattering amplitudes (4.7), (4.8) and (2.19). The analysis carried out so far proves the correctness of the RC method leading to the expected expressions for the form factor $Q^2 F_{\eta' g^* g^*}(Q^2, \omega)$ at $Q^2 \to \infty$ and demonstrating at the same time the consistency of the symmetrization of the hard-scattering amplitudes (2.29) and (2.30).

4.2 Contribution of the gluon component of the η'-meson to the form factor $F_{\eta' g^* g^*}(Q^2,\omega)$

The contribution of the gluon component of the η'-meson to the form factor $F_{\eta' g^* g^*}(Q^2,\omega)$ can be computed using the methods described in the previous subsection.

Using (2.30) for the hard-scattering amplitude $T_1^g(x,Q^2,\omega)$, (2.26) and the gluon component of the η'-meson DA, we have for the gluon part of the form factor

$$Q^2 F^g_{\eta' g^* g^*}(Q^2,\omega) = \frac{4\pi^2 C B(Q^2)}{3\beta_0}\int_0^\infty {\rm d}u e^{-ut} R(u,t) \tag{4.21}$$
$$\times\left[\int_0^1 {\rm d}x x^{1-u}\overline{x}(x-\overline{x})\frac{(1+\omega)x+(1-\omega)\overline{x}}{\omega\left[(1+\omega)\overline{x}+(1-\omega)x\right]}\right.$$
$$\left.+\int_0^1 {\rm d}x \overline{x}^{1-u}(x-\overline{x})\frac{(1+\omega)x+(1-\omega)\overline{x}}{\omega\left[(1+\omega)\overline{x}+(1-\omega)x\right]}\right],$$

which after some simple calculations becomes

$$Q^2 F^g_{\eta' g^* g^*}(Q^2,\omega) = \frac{4\pi^2 C B(Q^2)}{3\beta_0\omega}\int_0^\infty {\rm d}u e^{-ut} R(u,t)$$
$$\times\left\{B(4-u,2)\,{}_2F_1\left(1,4-u;6-u;\frac{2\omega}{1+\omega}\right)\right.$$
$$+B(4,2-u)\,{}_2F_1\left(1,4;6-u;\frac{2\omega}{1+\omega}\right)$$
$$-\frac{2\omega}{1+\omega}B(3,3-u)$$
$$\times\left[{}_2F_1\left(1,3-u;6-u;\frac{2\omega}{1+\omega}\right)\right.$$
$$\left.\left.+\,{}_2F_1\left(1,3;6-u;\frac{2\omega}{1+\omega}\right)\right]\right.$$
$$\left.-\frac{1-\omega}{1+\omega}\left[B(2-u,4)\,{}_2F_1\left(1,2-u;6-u;\frac{2\omega}{1+\omega}\right)\right.\right.$$
$$\left.\left.+B(2,4-u)\,{}_2F_1\left(1,2;6-u;\frac{2\omega}{1+\omega}\right)\right]\right\}. \tag{4.22}$$

For the η'-meson–on-shell-gluon transition, we find

$$Q^2 F^g_{\eta' g g^*}(Q^2,\omega=\pm 1) = \frac{4\pi^2 C B(Q^2)}{3\beta_0}\int_0^\infty {\rm d}u e^{-ut} R(u,t)$$
$$\times\left[B(1,4-u)+B(4,1-u)-B(2,3-u)\right.$$
$$\left.-B(3,2-u)\right], \tag{4.23}$$

or equivalently

$$Q^2 F^g_{\eta' g g^*}(Q^2,\omega=\pm 1) = \frac{4\pi^2 C B(Q^2)}{3\beta_0} \tag{4.24}$$
$$\int_0^\infty {\rm d}u e^{-ut} R(u,t)\left(\frac{1}{1-u}-\frac{4}{2-u}+\frac{4}{3-u}\right).$$

The form factor $Q^2 F^g_{\eta' g^* g^*}(Q^2,\omega=0)$ can be calculated by employing the following form for the hard-scattering amplitude:

$$T_1^g(x,Q^2,\omega) - T_2^g(x,Q^2,\omega) = \frac{2\pi}{3Q^2}\left[\alpha_{\rm s}(Q^2 x)+\alpha_{\rm s}(Q^2\overline{x})\right]\frac{x-\overline{x}}{1-\omega^2(x-\overline{x})^2}, \tag{4.25}$$

which for $\omega = 0$ leads to a very simple expression. Then, it is not difficult to demonstrate that

$$Q^2 F^g_{\eta' g^* g^*}(Q^2,\omega=0) = \frac{16\pi^2 C B(Q^2)}{3\beta_0} \tag{4.26}$$
$$\times\int_0^\infty {\rm d}u e^{-ut} R(u,t)$$
$$\times\left[B(4-u,2)-2B(3-u,3)+B(2-u,4)\right].$$

This latter expression can be recast into the form

$$Q^2 F^g_{\eta' g^* g^*}(Q^2,\omega=0) = \frac{16\pi^2 C B(Q^2)}{3\beta_0} \tag{4.27}$$
$$\times\int_0^\infty {\rm d}u e^{-ut} R(u,t)$$
$$\times\left[\frac{1}{2-u}-\frac{5}{3-u}+\frac{8}{4-u}-\frac{4}{5-u}\right].$$

The IR renormalon structure of the integrands in (4.24) and (4.27) is obvious: they have a finite number of IR renormalon poles located at the points $u_0 = 1,2,3$ and $u_0 = 2,3,4,5$, respectively. In order to find the IR renormalon structure of the integrand in (4.22), we expand the corresponding hypergeometric functions over $\beta = 2\omega/(1+\omega)$ in the region $\omega \in (0,1)$, providing the following result:

$$Q^2 F^g_{\eta' g^* g^*}(Q^2,\omega) = \frac{4\pi^2 C B(Q^2)}{3\beta_0\omega}$$

$$\times \int_0^\infty \mathrm{d}u \mathrm{e}^{-ut} R(u,t) \tag{4.28}$$
$$\times \sum_{k=0}^{\infty} \Big\{ \left[B(k+4,2-u)+B(k+4-u,2)\right]\beta^k$$
$$-\frac{1-\omega}{1+\omega}\left[B(k+2,4-u)+B(k+2-u,4)\right]\beta^k$$
$$-\left[B(k+3,3-u)+B(k+3-u,3)\right]\beta^{k+1}\Big\}.$$

Using the identities

$$B(k+4,2-u)=\frac{\Gamma(k+4)}{(2-u)(3-u)\dots(k+5-u)},$$
$$B(k+4-u,2)=\frac{1}{(k+4-u)(k+5-u)},$$
$$B(k+2,4-u)=\frac{\Gamma(k+2)}{(4-u)(5-u)\dots(k+5-u)},$$
$$B(k+2-u,4)=\frac{6}{(k+2-u)(k+3-u)(k+4-u)(k+5-u)},$$
$$B(k+3,3-u)=\frac{\Gamma(k+3)}{(3-u)(4-u)\dots(k+5-u)},$$
$$B(k+3-u,3)=\frac{2}{(k+3-u)(k+4-u)(k+5-u)}$$

it is easy to conclude that there is an infinite number of IR renormalon poles, being located at the points $u_0 = 2,3,\dots k+5$; $u_0 = k+4,\ k+5$; $u_0 = 4,5,\dots k+5$; $u_0 = k+2,\ k+3,\ k+4,\ k+5$; $u_0 = 3,4,\dots k+5$ and $u_0 = k+3,\ k+4,\ k+5$.

5 Numerical analysis

We begin this section by comparing the results obtained with the RC method with those from the IR matching scheme. In Sect. 3 we have noted that from experimental data only values of the non-perturbative parameters $f_1(2\,\mathrm{GeV})$ and $f_2(2\,\mathrm{GeV})$ have been extracted. We also know that the lowest-order moment integral and hence the parameter entering our formulas is $f_2(2\,\mathrm{GeV})$. Therefore, to make the comparison as clear as possible, we should choose the input parameters for the η'–virtual-gluon transition in such a way as to determine the behavior of the form factor solely with $f_2(2\,\mathrm{GeV})$. This can be easily achieved if we set for the η'-meson DA parameters

$$B_2^q(\mu_0^2)=0, \quad B_2^g(\mu_0^2)=0.$$

Under these circumstances, the gluon component of the vertex function vanishes. To remove from the analysis the higher-moment integrals $f_p(Q), p>2$, we consider only the η'-meson–on-shell-gluon transition, i.e., the $\omega=\pm1$ case. Moreover, we neglect the $\sim\alpha_s^2$ order term in (3.2) and set

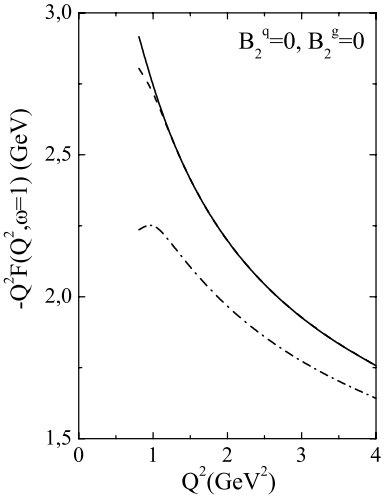

Fig. 3. Scaled $\eta' g$ transition form factor $-Q^2 F_{\eta' gg^*}(Q^2,\omega=\pm1)$ versus Q^2. The solid line is computed within the RC method, the dashed one is found using the IR matching scheme with $f_2(2\,\mathrm{GeV})\simeq 0.535$. The dot-dashed curve is obtained in the framework of the IR matching scheme using for $f_2(2\,\mathrm{GeV})$ the experimental value 0.5

in (3.8) $R(u,t)=1$ because in (3.19) α_s is used at the level of the one-loop order accuracy. After these simplifications, the FF is given by the following expression:

$$Q^2 F_{\eta' gg^*}(Q^2,\omega=\pm1) = -\frac{16\pi^2 C}{\beta_0}\int_0^\infty \frac{\mathrm{e}^{-ut}\mathrm{d}u}{1-u}$$
$$= -4\pi C f_2(Q). \tag{5.1}$$

Results of our computations are shown in Fig. 3, where, in order to distinguish the various curves, these are displayed in the region of $Q^2\in[1,4]\,\mathrm{GeV}^2$, whereas at higher Q^2 they are close to each other. The RC method and the IR matching scheme[5] both lead almost to identical predictions in the entire domain $1\,\mathrm{GeV}^2 \le Q^2 \le 25\,\mathrm{GeV}^2$, provided that in the IR matching scheme one uses in expression (3.19) the value $f_2(2\,\mathrm{GeV})\simeq 0.535$ found within the RC method (3.23). The curve following from the IR matching scheme deviates from the prediction obtained with the RC method only for $Q^2 < 1.4\,\mathrm{GeV}^2$. On the other hand, the deviation of that curve, calculated using the experimental value $f_2(2\,\mathrm{GeV})\simeq 0.5$, from the result of the RC method is sizeable in the region $Q^2 = 1\div 2\,\mathrm{GeV}^2$, reaching $\sim 30\%$ at $Q^2 = 1\,\mathrm{GeV}^2$. A similar behavior was observed in the calculation of the pion electromagnetic form factor, carried out within the context of these methods [61]. The difference between the solid and the dot-dashed lines in Fig. 3 is considerably reduced when varying the QCD scale parameter $\Lambda = 0.3\,\mathrm{GeV}$ or the experimental value of $f_2(2\,\mathrm{GeV})$ within their corresponding uncertainty limits. But we are not going to make decisive conclusions from these rather model-dependent calculations. Our aim here is to check and demonstrate that the RC method and

[5] Note that in the calculations within the IR matching scheme, (3.19) with $N=4$ has been used

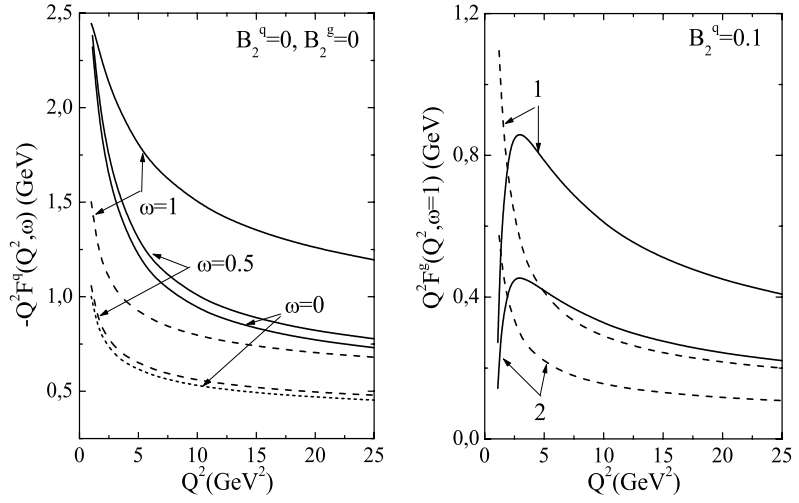

Fig. 4. The quark (left panel) and gluon (right panel) components of the transition form factor $Q^2 F^q_{\eta' g^* g^*}(Q^2, \omega)$ as functions of Q^2. The solid curves are obtained using the RC method, whereas the broken lines are calculated within the standard HSA. The quark component is computed at various ω values by employing the asymptotic DA. In the right panel the correspondence between the curves and the input parameter B_2^g is $B_2^g = 8$ for the curves labelled 1 and $B_2^g = 4$ for those labelled 2

the IR matching scheme predict in the considered region $1\,\mathrm{GeV}^2 \le Q^2 \le 25\,\mathrm{GeV}^2$ almost identical results that do not contradict experiment.

In order to proceed with the computation of the η'-meson–gluon vertex function and explore the role played by the η'–gluon content in this process, we have to define the allowed values of the free input parameters B_2^q and B_2^g at the normalization point $\mu_0^2 = 1\,\mathrm{GeV}^2$. These parameters determine the shape of the DAs of the quark and gluon components of the η'-meson and, in general, they have to be extracted from experimental data or computed by non-perturbative techniques. The comparison of the η'-meson–photon electromagnetic transition FF $F_{\eta'\gamma}(Q^2)$ with the CLEO data leads to the conclusion that the η'-meson DA must be close to its asymptotic form with a coefficient $B_2^q \simeq 0.1$ deduced in [6]. But this conclusion was made by neglecting the contribution of the gluon component of the η'-meson to the $\eta'\gamma$ transition FF. The investigation of the FF $F_{\eta'\gamma}(Q^2)$ was extended and revised in [62]. In fact, in this work the FF $F_{\eta'\gamma}(Q^2)$ was computed within the RC method by taking into account contributions arising due to both the quark and gluon components of the η'-meson DA. The comparison with the CLEO data demonstrated that allowed values of the Gegenbauer coefficients $B_2^q(1\,\mathrm{GeV}^2)$ and $B_2^g(1\,\mathrm{GeV}^2)$ are strongly correlated. They were extracted in [62] and read

$$B_2^q(1\,\mathrm{GeV}^2) = 0, \quad B_2^g(1\,\mathrm{GeV}^2) \in [4, 18],$$
$$B_2^q(1\,\mathrm{GeV}^2) = 0.05, \quad B_2^g(1\,\mathrm{GeV}^2) \in [0, 16], \quad (5.2)$$

and

$$B_2^q(1\,\mathrm{GeV}^2) = 0.1, \quad B_2^g(1\,\mathrm{GeV}^2) \in [-2, 14]. \quad (5.3)$$

In the present paper we select values of the parameters $B_2^q(1\,\mathrm{GeV}^2)$ and $B_2^g(1\,\mathrm{GeV}^2)$ that obey the constraints (5.2) and (5.3).

It is evident that the non-asymptotic terms in the quark and gluon DAs of the η'-meson proportional to $A(Q^2)$ and $B(Q^2)$, respectively, affect the asymptotic value of the η'-meson–gluon transition form factor. Therefore, before presenting contributions from these terms, it is instructive to study the asymptotic FF itself. In the left panel of Fig. 4, we depict the η'-meson–virtual-gluon transition FF as a function of the gluon virtuality Q^2. For the asymptotic DA the quark component of the form factor coincides with the full one. In the same figure the predictions obtained within the standard HSA are also shown. One sees that in the domain $1\,\mathrm{GeV}^2 \le Q^2 \le 25\,\mathrm{GeV}^2$ the standard pQCD results get enhanced by approximately a factor of 2 due to power corrections. A similar conclusion is valid also for the gluon component of the form factor (right panel in Fig. 4, computed by employing the η'-meson DAs).

Here some comments concerning the accuracy of the numerical computations are in order. In Fig. 4 (left panel) and in the following ones, the curves obtained within the RC method, as a rule, require a summation of an infinite series. In real numerical computations we truncate such a series at some $k = K_{\max}$. Naturally, the question arises about the convergence rate of this series. Let us explain this problem by considering Fig. 4 as an example. The solid curve with $\omega = 0.5$ in Fig. 4 (left panel) has been found within the RC method by employing (4.12). This expression contains a series with factorially growing coefficients. For definiteness we analyze the term

$$\int_0^\infty \mathrm{d}u e^{-ut} R(u,t) \sum_{k=0}^{\infty} B(k+2, 2-u)\beta^k$$
$$= \sum_{k=0}^{\infty} \int_0^\infty \mathrm{d}u e^{-ut} R(u,t)$$
$$\times \frac{\Gamma(k+2)}{(2-u)(3-u)\ldots(k+3-u)} \beta^k. \quad (5.4)$$

The expansion parameter $\beta = 2\omega/(1+\omega)$ in (5.4) at the point $\omega = 0.5$ is equal to $\beta = 2/3$. Below, we write down the values of the Gamma function $\Gamma(k+2) = (k+1)!$ and also those of the product of β^k with the principal value of

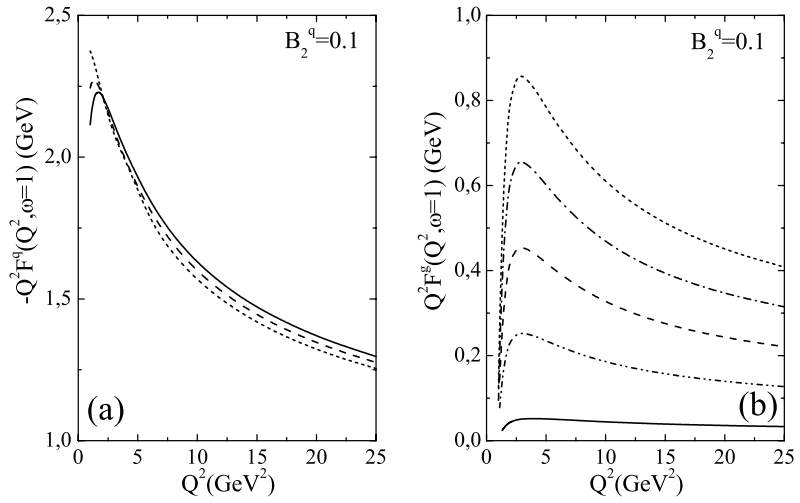

Fig. 5. The contribution of the quark **a** and gluon **b** components of the η' meson to the form factor $Q^2 F_{\eta' gg^*}(Q^2, \omega = \pm 1)$ versus Q^2. All curves are obtained in the context of the RC method. The correspondence between all displayed curves and the parameter B_2^g is $B_2^g = 0$ for the solid curves; $B_2^g = 2$ for the dot-dot-dashed curve; $B_2^g = 4$ for the dashed lines; $B_2^g = 6$ for the dot-dashed line, and $B_2^g = 8$ for the short-dashed curves. In **a** curves corresponding only to $B_2^g = 0$, 4 and 8 are shown

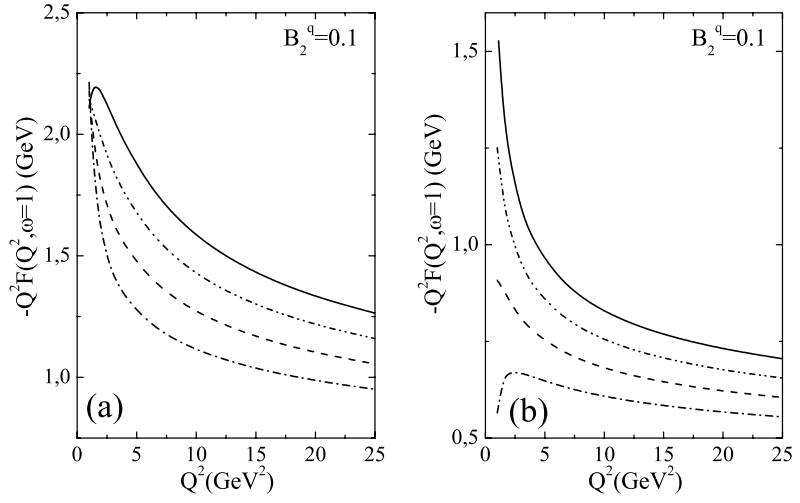

Fig. 6. The form factor $-Q^2 F_{\eta' gg^*}(Q^2, \omega = \pm 1)$ computed using the RC method **a** and the standard HSA **b**. The correspondence between displayed curves and the parameter B_2^g is $B_2^g = 0$ for solid curves; $B_2^g = 2$ for the dot-dot-dashed curves; $B_2^g = 4$ for the dashed lines; $B_2^g = 6$ for the dot-dashed lines

the integral

$$I(k) = \int_0^\infty \mathrm{d}u \mathrm{e}^{-ut} R(u,t) \frac{\beta^k}{(2-u)(3-u)\dots(k+3-u)}, \tag{5.5}$$

for $k = 0$, 5 and 10,

$$\Gamma(2) = 1, \quad \Gamma(7) = 720, \quad \Gamma(12) = 3.99168 \cdot 10^7,$$

and

$$I(0) \simeq 0.09041, \quad I(5) \simeq 2.44061 \cdot 10^{-6},$$
$$I(10) \simeq 1.31568 \cdot 10^{-12}\ .$$

As a result, the corresponding terms in the sum given by (5.4) take the values

$$0.09041, \quad 1.75724 \cdot 10^{-3}, \quad 5.25177 \cdot 10^{-5},$$

respectively. The calculations above have been performed at $Q^2 = 2\,\mathrm{GeV}^2$. At the momentum transfer $Q^2 = 20\,\mathrm{GeV}^2$ we get

$$0.03898, \quad 7.59618 \cdot 10^{-4}, \quad 4.42997 \cdot 10^{-5}.$$

One observes that the convergence rates of the numerical series are high and that we can therefore truncate them, as a rule, at $K_{\max} = 20$.

We have analyzed the impact of the various DAs of the η'-meson on the $\eta' g$ transition form factor. The quark component of the FF is stable for different values of $B_2^g \in [0, 8]$. It is difficult to distinguish the corresponding curves and therefore in Fig. 5a we can only plot some of them. In contrast, the gluon component of the form factor demonstrates a rapid growth with B_2^g (Fig. 5b). As a result, due to different signs of the quark and gluon components of the space-like vertex function, the total vertex function $Q^2 F_{\eta' gg^*}(Q^2, \omega = \pm 1)$ for $B_2^g \neq 0$ lies below the asymptotic one (Fig. 6a). Comparing the predictions derived within the RC method with those following from the standard HSA (Fig. 6b), we see a quantitative difference between corresponding curves.

The dependence of the quark and gluon components of the form factor on the asymmetry parameter ω at fixed Q^2 and for various DAs of the η'-meson are shown in Fig. 7. Because $F_{\eta' g^* g^*}(Q^2, \omega)$ is symmetric under the exchange $\omega \leftrightarrow -\omega$, we present our results in the region $0 \leq \omega \leq 1$ only. We have just demonstrated in Fig. 5 that the quark component of the FF $F^q_{\eta' gg^*}(Q^2, \omega = \pm 1)$ is not sensitive

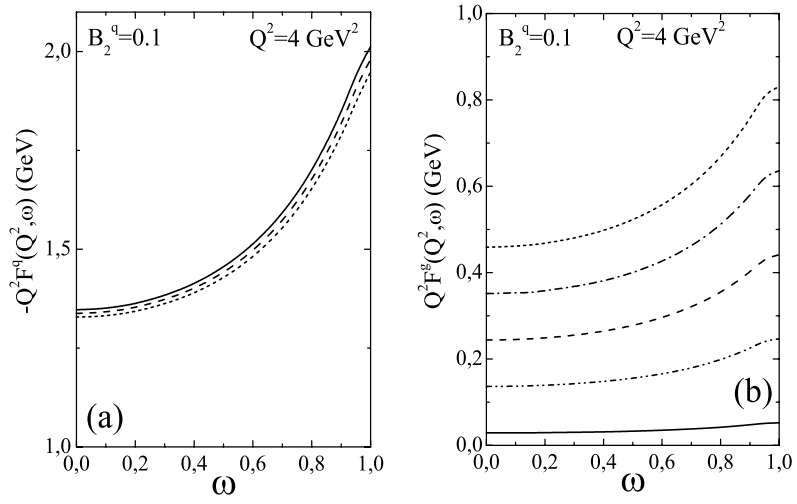

Fig. 7. The quark **a** and gluon **b** components of the FF at fixed total gluon virtuality $Q^2 = 4\,\mathrm{GeV}^2$ as functions of the asymmetry parameter ω. The RC method is employed. The correspondence between depicted lines and the parameter B_2^g is the same as in Fig. 5

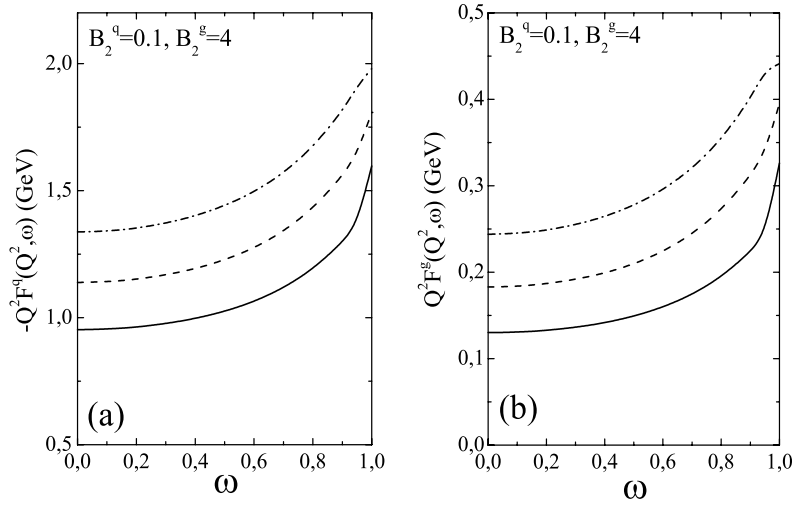

Fig. 8. The quark **a** and gluon **b** components of the form factor $Q^2 F_{\eta' g^* g^*}(Q^2, \omega)$ at fixed Q^2 versus ω. The RC method is used. The momentum scale for the solid curves $Q^2 = 10\,\mathrm{GeV}^2$, for the dashed ones $Q^2 = 6\,\mathrm{GeV}^2$, and for the dot-dashed curves $Q^2 = 4\,\mathrm{GeV}^2$

to the use of various η'-meson DAs, employed in our calculations. This is valid also for its behavior as a function of ω (Fig. 7a). In accordance with our computations, the effect of the chosen parameter B_2^g on the gluon component of the FF is considerable in the whole range of $\omega \in [0, 1]$.

The magnitude of the quark and gluon components of the form factor for a given DA depends on the total gluon virtuality Q^2 (Fig. 8). In this case both the quark and gluon contributions to the FF demonstrate sensitivity to the fixed value of Q^2.

The features of the quark and gluon components of the $\eta' g^*$ transition FF described above determine the behavior of their sum as a function of the asymmetry parameter ω and, as a result, we get the picture shown in Fig. 9a. Owing to the gluon component, the form factor $F_{\eta' g^* g^*}(Q^2, \omega)$ depends on the η'-meson DA used in the calculations. For comparison, in Fig. 9b the curves found within the standard HSA are also shown. An enhancement of about a factor of 2 of the vertex function due to power corrections is evident.

The $\eta' g^*$ transition FF as a function of the first gluon virtuality Q_1^2 at various fixed values of the second one, Q_2^2, and for different DAs is plotted in Fig. 10.

As we have noted in Sect. 3, the principal value prescription, adopted in this work to regularize divergent integrals, produces higher-twist ambiguities. It is important to clarify to what extent these ambiguities may alter our predictions. To illustrate this effect, we depict in Fig. 11, as an example, the scaled $\eta' g$ transition FF $Q^2 F_{\eta' g g^*}(Q^2, \omega = \pm 1)$. The higher-twist ambiguities lead approximately to $\pm 15\%$ shifts relative to the previous RC result (line 2). On the other hand, comparing the standard pQCD prediction (solid line 1) with the lower dashed line (that denotes the RC prediction with a negative higher-twist ambiguity), we see that still the power corrections provide an enhancement of the standard pQCD result by a factor ~ 2 in the region $Q^2 \sim 1$–$2\,\mathrm{GeV}^2$ and by a factor ~ 1.6 at $Q^2 = 25\,\mathrm{GeV}^2$. This latter effect is connected not only to larger uncertainties, but it also reflects the general trend of the FF to reach its asymptotic value, i.e., the line 1 in the limit $Q^2 \to \infty$.

6 Concluding remarks

In this paper we have evaluated power-suppressed corrections $\sim 1/Q^{2n},\ n = 1, 2, \ldots$ to the space-like η'-meson–virtual-gluon transition form factor $Q^2 F_{\eta' g^* g^*}(Q^2, \omega)$. To this end, we have employed the standard hard-scattering approach and the running coupling method in conjunc-

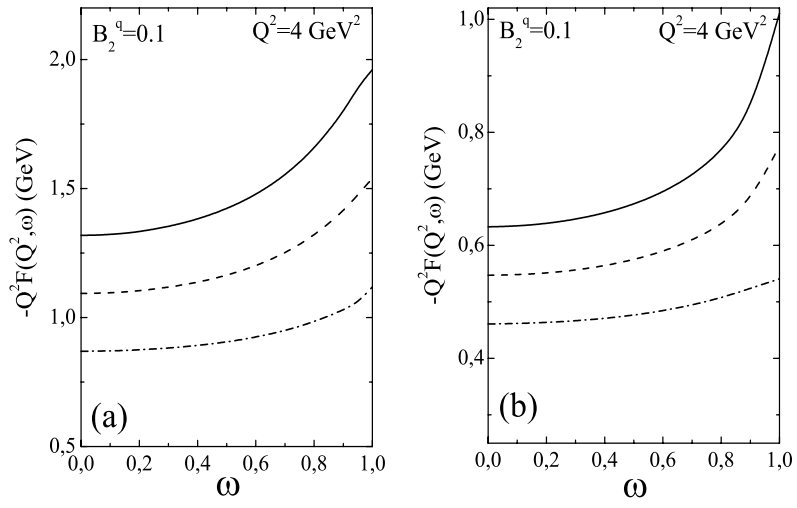

Fig. 9. The FF $-Q^2 F_{\eta' g^* g^*}(Q^2,\omega)$ obtained by employing the RC method **a** and the standard HSA **b** as a function of ω. The expansion coefficients are $B_2^g = 0$ for the solid lines, $B_2^g = 4$ for the dashed lines, and $B_2^g = 8$ for the dot-dashed lines

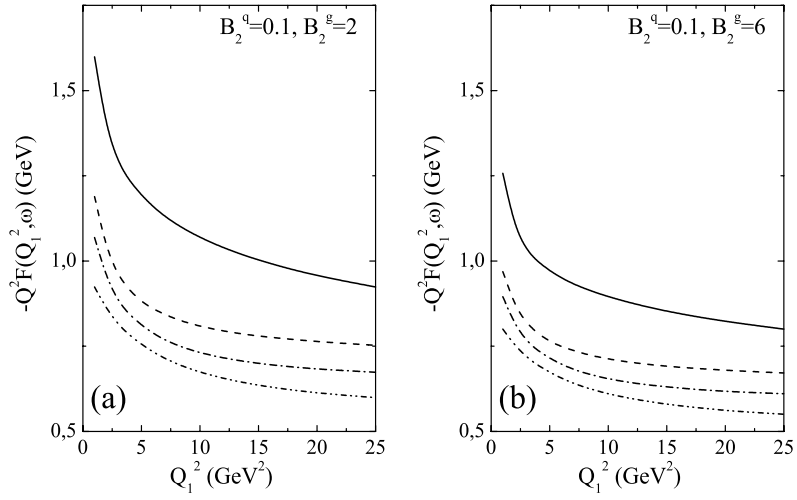

Fig. 10. The form factor $-Q^2 F_{\eta' g^* g^*}(Q_1^2,\omega)$ for two different DAs of the η' meson and at different fixed values of Q_2^2; viz., for the solid curves $Q_2^2 = 1\,\mathrm{GeV}^2$, for the dashed curves $Q_2^2 = 5\,\mathrm{GeV}^2$, for the dot-dashed curves $Q_2^2 = 10\,\mathrm{GeV}^2$, and for the dot-dot-dashed curves $Q_2^2 = 25\,\mathrm{GeV}^2$

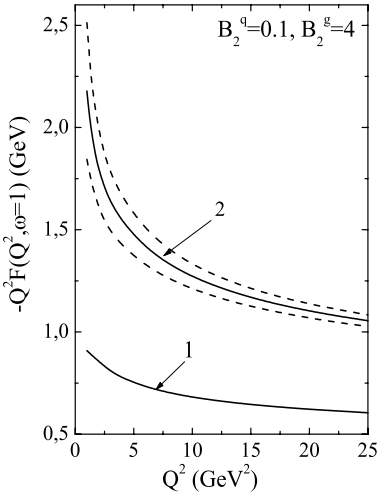

Fig. 11. Influence of higher-twist ambiguities on the form factor $-Q^2 F_{\eta' g g^*}(Q^2, \omega = \pm 1)$, calculated with the RC method (broken lines). The solid lines, labelled 1 and 2, correspond to the FF found before within perturbative QCD and the RC method, respectively. For the upper dashed line the constants determining the ambiguities are taken to be equal to $\{N_q\} = 1$, while for the lower dashed line $\{N_q\} = -1$, where $q = 1, 2$ and 3

tion with the infrared renormalon calculus. In the calculations, both the quark and the gluon distribution amplitudes of the η' meson have been taken into account. In these model DAs only the first non-asymptotic terms have been retained and the values of the input coefficients $B_2^q(1\,\mathrm{GeV}^2)$ and $B_2^g(1\,\mathrm{GeV}^2)$ extracted from the analysis of the CLEO data on the $\eta'\gamma$ electromagnetic transition FF have been employed.

In order to apply the RC method to the considered process, the hard-scattering amplitudes of the corresponding subprocesses have been generalized in such a way as to preserve the symmetry properties of both the hard-scattering amplitudes and the transition form factor itself under the replacements $x \leftrightarrow \overline{x}$ and $\omega \leftrightarrow -\omega$. In the computations within the RC method, the Laplace transformed expression for the running coupling has been employed. The Borel resummed form factors, obtained this way, have been regularized by means of the principal value prescription. Various limits of the general expression $Q^2 F_{\eta' g^* g^*}(Q^2,\omega)$ have been found.

Our expressions for the vertex function $F_{\eta' g^* g^*}(Q^2,\omega)$, found within the standard HSA, are in agreement with corresponding predictions made in [26] (up to a conventional sign factor). It has been demonstrated that (see (2.27))

both the quark and the gluon components of the vertex function are symmetric under the exchange $\omega \leftrightarrow -\omega$, as they must be owing to the Bose symmetry of the final gluons. The RC method has provided us a tool for estimating power corrections to the vertex function $F_{\eta' g^* g^*}(Q^2,\omega)$. These corrections are implicitly contained in the pQCD factorization formulas (2.14) and (2.15) and originate from the end-point $x \to 0;1$ regions. It is clear that such corrections cannot been taken into account in the standard pQCD approach by freezing the renormalization scale $\mu_{\rm R}^2$ and ignoring its dependence on the longitudinal momentum fraction x. As an important consistency check, we have proven that the results obtained with the RC method in the asymptotic limit $Q^2 \to \infty$ reproduce the standard pQCD predictions for the vertex function. This provides further justification for the treatment of the hard-scattering amplitudes (2.29) and (2.30), and the symmetrization procedure employed in the running coupling method.

The presented numerical analysis shows that power corrections considerably enhance the standard pQCD predictions for the form factor in the explored region $1\,\mathrm{GeV}^2 \le Q^2 \le 25\,\mathrm{GeV}^2$, though other sources, not considered here, may also give rise to power corrections. Our investigations demonstrate that the quark component of the form factor at fixed $B_2^q = 0.1$ is practically stable for several values of $B_2^g = 0,\ 2,\ 4,\ 6,\ 8$. Contrary to this, the gluon component of the FF is sensitive to the adopted value of B_2^g. As a consequence, the $\eta' g^*$ transition FF was found to depend on the gluonic content of the η' meson. In the considered region the gluon contribution reduces the absolute value of the space-like form factor $Q^2 F_{\eta' g^* g^*}(Q^2,\omega)$.

As is true of any technique for calculating power corrections, the theoretical framework elaborated in the present work makes assumptions about the regularization of the end-point divergences. There are of course other possibilities. Nevertheless, we believe that our method is useful in pQCD analyses of the B-meson exclusive decays and heavy-to-light $B \to \pi, \rho$ transition form factors in the domain of moderate momentum transfers. A generalization of the RC method to describe time-like transitions as well as its combination with resummation techniques to include Sudakov logarithms will be the subject of separate investigations.

Acknowledgements. One of the authors (S.S.A.) would like to thank Prof. S. Randjbar-Daemi and the High Energy Section members for their hospitality at the Abdus Salam ICTP, where this work was started and Prof. K. Goeke and the members of the Institute for Theoretical Physics II, where this investigation was completed. Both of us wish to thank M. Polyakov, A. Bakulev, A. Belitsky, and K. Passek-Kumerički for useful comments. The financial support by DAAD (S.S.A.) is gratefully acknowledged.

Appendix

In this appendix we collect expressions for the η'-meson quark and gluon DAs for $n_f = 4$. The parameters (2.38) which determine these DAs assume the following values:

$$\gamma_{gg}^2 = -\frac{35}{3},\ \gamma_{qg}^2 = 4,\ \gamma_+^2 \simeq -\frac{48}{9}, \quad \gamma_-^2 \simeq -\frac{107}{9},$$
$$\rho_2^q \simeq \frac{19}{5},\ \rho_2^g \simeq -\frac{1}{102}.$$

It is evident that the elements of the anomalous dimensions matrix γ_{qq}^2 and γ_{gq}^2 are n_f independent and have the values shown in (2.38).

In the $n_f = 4$ case the DAs $\phi^q(x,Q^2)$ and $\phi^g(x,Q^2)$ of the η'-meson have the form (2.39) as well, the only difference being in the functions $A(Q^2)$ and $B(Q^2)$, which now are defined by the expressions

$$A(Q^2) = 6B_2^q \left(\frac{\alpha_{\rm s}(Q^2)}{\alpha_{\rm s}(\mu_0^2)}\right)^{\frac{48}{75}} - \frac{B_2^g}{17}\left(\frac{\alpha_{\rm s}(Q^2)}{\alpha_{\rm s}(\mu_0^2)}\right)^{\frac{107}{75}},$$
$$B(Q^2) = 19B_2^q \left(\frac{\alpha_{\rm s}(Q^2)}{\alpha_{\rm s}(\mu_0^2)}\right)^{\frac{48}{75}} + 5B_2^g\left(\frac{\alpha_{\rm s}(Q^2)}{\alpha_{\rm s}(\mu_0^2)}\right)^{\frac{107}{75}}. \tag{A.1}$$

In the previous sections all results have been written down for $n_f = 3$ valid for momentum transfers $1\,\mathrm{GeV}^2 \le Q^2 < 2\,\mathrm{GeV}^2$. For momentum transfers in the range $2\,\mathrm{GeV}^2 \le Q^2 \le 25\,\mathrm{GeV}^2$, the choice $n_f = 4$ has to be employed. In this case, the expressions that determine the quark component of the transition FF remain unchanged, except for the function $A(Q^2)$ (and β_0, $R(u,t)$), which should be taken from (A.1). The expressions for the gluon component of the FF have to be rescaled by a factor $3/4$ – apart from the replacement of the function $B(Q^2)$ (and β_0, $R(u,t)$) – since the hard-scattering amplitudes $T_{1(2)}^g(x,Q^2,\omega)$ explicitly depend on n_f (2.30).

References

1. CLEO Collaboration, J. Gronberg et al., Phys. Rev. D **57**, 33 (1998) [hep-ex/9707031]
2. CLEO Collaboration, B.H. Behrens et al., Phys. Rev. Lett. **80**, 3710 (1998) [hep-ex/9801012]; T.E. Browder et al., Phys. Rev. Lett. **81**, 1786 (1998) [hep-ex/9804018]
3. J. Cao, F.-G. Cao, T. Huang, B.-Q. Ma, Phys. Rev. D **58**, 113006 (1998) [hep-ph/9807508]
4. R. Jakob, P. Kroll, M. Raulfs, J. Phys. G **22**, 45 (1996) [hep-ph/9410304]
5. Th. Feldmann, P. Kroll, Eur. Phys. J. C **5**, 327 (1998) [hep-ph/9711231]
6. S.S. Agaev, Phys. Rev. D **64**, 014007 (2001)
7. M.K. Chase, Nucl. Phys. B **174**, 109 (1980)
8. M.V. Terentev, Sov. J. Nucl. Phys. **33**, 911 (1981) [Yad. Fiz. **33**, 1692 (1981)]
9. T. Ohrndorf, Nucl. Phys. B **186**, 153 (1981)
10. M.A. Shifman, M.I. Vysotsky, Nucl. Phys. B **186**, 475 (1981)
11. V.N. Baier, A.G. Grozin, Nucl. Phys. B **192**, 476 (1981)

12. D. Atwood, A. Soni, Phys. Lett. B **405**, 150 (1997) [hep-ph/9704357]
13. W.-S. Hou, B. Tseng, Phys. Rev. Lett. **80**, 434 (1998) [hep-ph/9705304]
14. A.L. Kagan, A.A. Petrov, hep-ph/9707354
15. M. Ahmady, E. Kou, A. Sugamoto, Phys. Rev. D **58**, 014015 (1998) [hep-ph/9710509]
16. A. Ali, J. Chay, C. Greub, P. Ko, Phys. Lett. B **424**, 161 (1998) [hep-ph/9712372]; D. Du, C.S. Kim, Y. Yang, Phys Lett. B **426**, 133 (1998) [hep-ph/9711428]
17. I. Halperin, A. Zhitnitsky, Phys. Rev. D **56**, 7247 (1997) [hep-ph/9704412]; Phys. Rev. Lett. **80**, 438 (1998) [hep-ph/9705251]
18. M. Franz, P.V. Pobylitsa, M.V. Polyakov, K. Goeke, Phys. Lett. B **454**, 335 (1999) [hep-ph/9810343]; M. Franz, M.V. Polyakov, K. Goeke, Phys. Rev. D **62**, 074024 (2000) [hep-ph/0002240]
19. A.S. Dighe, M. Gronau, J. Rosner, Phys. Lett. B **367**, 357 (1996) [Erratum B **377**, 325 (1996)] [hep-ph/9509428]; H. Fritzsch, Phys. Lett. B **415**, 83 (1997) [hep-ph/9708348]; A. Datta, X.-G. He, S. Pakvasa, Phys. Lett. B **419**, 369 (1998) [hep-ph/9707259]; X.-G. He, G.-L. Lin, Phys. Lett. B **454**, 123 (1999) [hep-ph/9809204]; T.W. Yeh, H.-n. Li, Phys. Rev. D **56**, 1656 (1997) [hep-ph/9701233]; H.-n. Li, B. Tseng, Phys. Rev. D **57**, 443 (1997) [hep-ph/9706441]; M.R. Ahmady, E. Kou, Phys. Rev. D **59**, 054014 (1999) [hep-ph/9807398]
20. J.O. Eeg, A. Hiorth, A.D. Polosa, Phys. Rev. D **65**, 054030 (2002) [hep-ph/0109201]; E. Kou, A.I. Sanda, Phys. Lett. B **525**, 240 (2002) [hep-ph/0106159]; A. Deandrea, A.D. Polosa, Eur. Phys. J. C **22**, 677 (2002) [hep-ph/0107234]; Y.Y. Keum, H.-n. Li, A.I. Sanda, Phys. Rev. D **63**, 054008 (2001) [hep-ph/0004173]; Y.Y. Keum, H.-n. Li, Phys. Rev. D **63**, 074006 (2001) [hep-ph/0006001]; Y.Y. Keum, Preprint DPNU-02-33 [hep-ph/0210127]
21. M. Beneke, G. Buchalla, M. Neubert, C.T. Sachrajda, Phys. Rev. Lett. **83**, 1914 (1999) [hep-ph/9905312]; Nucl. Phys. B **591**, 313 (2000) [hep-ph/0006124]; B **606**, 245 (2001) [hep-ph/0104110]
22. M. Beneke, M. Neubert, Nucl. Phys. B **651**, 225 (2003) [hep-ph/0210085]
23. T. Muta, M.-Z. Yang, Phys. Rev. D **61**, 054007 (2000) [hep-ph/9909484]
24. M.-Z. Yang, Y.-D. Yang, Nucl. Phys. B **609**, 469 (2001) [hep-ph/0012208]
25. A. Ali, A. Ya. Parkhomenko, Phys. Rev. D **65**, 074020 (2002) [hep-ph/0012212]
26. P. Kroll, K. Passek-Kumerički, Phys. Rev. D **67**, 054017 (2003) [hep-ph/0210045]
27. G.P. Lepage, S.J. Brodsky, Phys. Rev. D **22**, 2157 (1980); A.V. Efremov, A.V. Radyushkin, Phys. Lett. B **94**, 245 (1980); Theor. Math. Phys. **42**, 97 (1980) [Teor. Mat. Fiz. **42**, 147 (1980)]; A. Duncan, A.H. Mueller, Phys. Rev. D **21**, 1636 (1980)
28. M. Beneke, Phys. Rep. **317**, 1 (1999) [hep-ph/9807443]
29. S.J. Brodsky, G.P. Lepage, P.B. Mackenzie, Phys. Rev. D **25**, 228 (1983)
30. S.S. Agaev, Phys. Lett. B **360**, 117 (1995) [Erratum B **369**, 379 (1996)]; Mod. Phys. Lett. A **10**, 2009 (1995); A **11**, 957 (1996); A **13**, 2637 (1998) [hep-ph/9805278]
31. S.S. Agaev, A.I. Mukhtarov, Y.V. Mamedova, Mod. Phys. Lett. A **15**, 1419 (2000)
32. P. Gosdzinsky, N. Kivel, Nucl. Phys. B **521**, 274 (1998) [hep-ph/9707367]; S.S. Agaev, A.I. Mukhtarov, Int. J. Mod. Phys. A **16**, 3179 (2001)
33. D.V. Shirkov, I.L. Solovtsov, Phys. Rev. Lett. **79**, 1209 (1997) [hep-ph/9704333]
34. A.I. Karanikas, N.G. Stefanis, Phys. Lett. B **504**, 225 (2001) [hep-ph/0101031]
35. N.G. Stefanis, in 8th Adriatic Meeting and Central European Symposia on Particle Physics in the New Millennium, Dubrovnik, Croatia, 4–14 September 2001, published in Lect. Notes Phys. **616**, 153 (2003) [hep-ph/0203103]
36. A.A. Petrov, Phys. Rev. D **58**, 054004 (1998) [hep-ph/9712497]
37. E. Kou, Phys. Rev. D **63**, 054027 (2001) [hep-ph/9908214]
38. KLOE Collaboration, A. Aloisio et al., Phys. Lett. B **541**, 45 (2002) [hep-ex/0206010]
39. Th. Feldmann, P. Kroll, B. Stech, Phys. Lett. B **449**, 339 (1999) [hep-ph/9812269]
40. Th. Feldmann, P. Kroll, B. Stech, Phys. Rev. D **58**, 114006 (1998) [hep-ph/9802409]
41. H. Leutwyler, Nucl. Phys. (Proc. Suppl.) **64**, 223 (1998) [hep-ph/9709408]; R. Kaiser, H. Leutwyler, hep-ph/9806336
42. Th. Feldmann, Int. J. Mod. Phys. A **15**, 159 (2000) [hep-ph/9907491]
43. N.G. Stefanis, W. Schroers, H.C. Kim, Eur. Phys. J. C **18**, 137 (2000) [hep-ph/0005218]
44. R.D. Field, R. Gupta, S. Otto, L. Chang, Nucl. Phys. B **186**, 429 (1981)
45. F.-M. Dittes, A.V. Radyushkin, Sov. J. Nucl. Phys. **34**, 293 (1981) [Yad. Fiz. **34**, 529 (1981)]; E. Braaten, S.-M. Tse, Phys. Rev. D **35**, 2255 (1987)
46. F. del Aguila, M.K. Chase, Nucl. Phys. B **193**, 517 (1981); E. Braaten, Phys. Rev. D **28**, 524 (1983); E.P. Kadantseva, S.V. Mikhailov, A.V. Radyushkin, Sov. J. Nucl. Phys. **44**, 326 (1986) [Yad. Fiz. **44**, 507 (1986)]; B. Nižić, Phys. Rev. D **35**, 80 (1987); B. Melić, B. Nižić, K. Passek, Phys. Rev. D **65**, 053020 (2002) [hep-ph/0107295]
47. A.P. Bakulev, S.V. Mikhailov, N.G. Stefanis, Phys. Lett. B **508**, 279 (2001) [hep-ph/0103119]; hep-ph/0104290; Phys. Rev. D **67**, 074012 (2003) [hep-ph/0212250]; Preprint RUB-TPII-04/03 [hep-ph/0303039], to be published in Phys. Lett. B
48. A.V. Belitsky, D. Müller, Nucl. Phys. B **537**, 397 (1999) [hep-ph/9804379]
49. H. Bateman, A. Erdélyi, Higher transcendental functions (McGraw-Hill, New York 1953), Vol. 2
50. H. Contopanagos, G. Sterman, Nucl. Phys. B **419**, 77 (1994) [hep-ph/9310313]
51. G. 't Hooft, in The Whys of Subnuclear Physics, Proceedings of the International School, Erice, 1977, edited by A. Zichichi (Plenum, New York 1978); V.I. Zakharov, Nucl. Phys. B **385**, 452 (1992)
52. H. Bateman, A. Erdélyi, Tables of integral transforms (McGraw-Hill, New York 1954), Vol. 1
53. B.R. Webber, JHEP **9810**, 012 (1998) [hep-ph/9805484]
54. M. Dasgupta, G.P. Salam, JHEP **0208**, 032 (2002) [hep-ph/0208073]
55. P.A. Movilla Fernández, S. Bethke, O. Biebel, S. Kluth, Eur. Phys. J. C **22**, 1 (2001) [hep-ex/0105059]
56. H1 Collaboration, C. Adloff et al., Eur. Phys. J. C **14**, 255 (2000) [Erratum C **18**, 417 (2000)] [hep-ex/9912052]

57. New Muon Collaboration, M. Arneodo et al., Nucl. Phys. B **483**, 3 (1997); CCFR/NuTeV Collaboration, W.G. Seligman et al., Phys. Rev. Lett. **79**, 1213 (1997); M. Virchaux, A. Milsztajn, Phys. Lett. B **274**, 221 (1992); A.L. Kataev, A.V. Kotikov, G. Parente, A.V. Sidorov, Phys. Lett. B **417**, 374 (1998) [hep-ph/9706534]
58. M. Dasgupta, B.R. Webber, Phys. Lett. B **382**, 273 (1996) [hep-ph/9604388]; Nucl. Phys. B **484**, 247 (1997) [hep-ph/9608394]
59. A.P. Prudnikov, Yu.A. Brychkov, O.I. Marichev, Integrals and series, Vol. 1: Elementary functions (Gordon and Breach, New York 1986)
60. A.P. Prudnikov, Yu.A. Brychkov, O.I. Marichev, Integrals and series, Vol. 3: More special functions (Gordon and Breach, New York 1990)
61. S.S. Agaev, Nucl. Phys. B (Proc. Suppl.) **74**, 155 (1999) [hep-ph/9807444]
62. S.S. Agaev, N.G. Stefanis, Preprint RUB-TPII-09/03 [hep-ph/0307087]